# EFFECTS OF INTERMITTENT HYPOXIA ON THE CELL SURVIVAL AND INFLAMMATORY RESPONSES IN THE INTERTIDAL MARINE BIVALVES *MYTILUS EDULIS* AND *CRASSOSTREA GIGAS*

Halina Falfushynska[1,2], Helen Piontkivska[3], and Inna M. Sokolova[1,4]*

[1]Department of Marine Biology, Institute of Biological Sciences, University of Rostock, Rostock, Germany

[2]Department of Human Health, Physical Rehabilitation and Vital Activity, Ternopil V. Hnatiuk National Pedagogical University, Ternopil, Ukraine

[3]Department of Biological Sciences, Kent State University, Kent, OH, USA

[4]Department of Maritime Systems, Interdisciplinary Faculty, University of Rostock, Rostock, Germany

*Corresponding author: Inna Sokolova, inna.sokolova@uni-rostock.de

**ABSTRACT.** Hypoxia is a major stressor in estuarine and coastal habitats leading to adverse effects in aquatic organisms. Estuarine bivalves such as the blue mussels *Mytilus edulis* and the Pacific oysters *Crassostrea gigas* can survive periodic oxygen deficiency but the molecular mechanisms that underlie cellular injury during hypoxia-reoxygenation are not well understood. We examined the molecular markers of autophagy, apoptosis and inflammation during the short-term (1 day) and long-term (6 days) hypoxia and post-hypoxic recovery (1 h) in the mussels and oysters by measuring the lysosomal membrane stability, activity of a key autophagic enzyme (cathepsin D) and mRNA expression of the genes involved in the cellular survival and inflammation, including caspases 2, 3 and 8, Bcl-2, BAX, TGF-β-activated kinase 1 (TAK1), nuclear factor kappa B-1 (NF-κB), and NF-κB activating kinases IKKα and TBK1. C *gigas* exhibited higher hypoxia tolerance as well as blunted or delayed inflammatory and apoptotic response to hypoxia and reoxygenation shown by the later onset and/or the lack of transcriptional activation of caspases, BAX and an inflammatory effector NF-κB compared with *M.edulis*. Long-term hypoxia resulted in upregulation of Bcl-2 in the oysters and the mussels implying activation of the anti-apoptotic mechanisms. Our findings indicate the potential importance of the cell survival pathways in hypoxia tolerance of marine bivalves and demonstrate the utility of the molecular markers of apoptosis and autophagy for assessment of the sublethal hypoxic stress in bivalve populations.

## INTRODUCTION

Hypoxia (i.e. oxygen deficiency) and anoxia (the lack of oxygen) are major stressors for aquatic organisms that experience fluctuations in the oxygen availability due to the natural oxygen cycles as well as the human-driven deoxygenation of aquatic habitats due to eutrophication and warming (Breitburg et al., 2018). In estuaries and coastal habitats, hypoxia is common and can last from a few hours (such as during the tidal emersion or diel cycles of photosynthesis and respiration) to weeks to months (such as during seasonal hypoxia in eutrophicated estuaries) (Breitburg et al., 2018). Prolonged or permanent hypoxia is lethal for most metazoans, so that hypoxia is considered a major driver of biodiversity loss in aquatic habitats (Chu et al.; Levin et al., 2009). Sessile benthic organisms are especially sensitive to the coastal hypoxia due to their inability to escape the deoxygenated bottom water and sediments (Chu et al.; Levin et al., 2009). However, some benthic marine organisms, including intertidal bivalves, are exceptionally well adapted to survive periodic oxygen deficiency and can withstand days to weeks of hypoxia and anoxia, depending on the temperature (Babarro and De Zwaan, 2008; Diaz and Rosenberg, 2008). A major adaptive strategy for hypoxia survival in these organisms is an ability to suppress the rate of the ATP turnover well below the normoxic level, sometimes down to < 5% of the standard aerobic metabolic rate (Guppy and Withers, 1999; Shick et al., 1983; Sokolova et al., 2000; Storey and Storey, 2004). This metabolic avoidance strategy of coordinated suppression of ATP consumption and ATP production, called metabolic rate depression, slows down accumulation of potentially toxic end products and helps to conserve the energy reserves (Hochachka et al., 1996; Hochachka and Guppy, 1987; Hochachka and Mommsen, 1983). These adaptations can slow down but do not fully prevent the deterioration of the cellular homeostasis, especially during prolonged hypoxia.

The metabolic rate depression is effective in extending the survival time during hypoxia and anoxia. However, it is a time-limited situation that requires the return of oxygen for an organism to recover and complete the life cycle. The post-hypoxic reoxygenation presents an additional host of problems to aerobic organisms because of the energy costs associated with the reinstatement of the cellular homeostasis and increased biosynthesis to replenish the energy reserves (Bayne, 2017; Ellington, 1983; Lewis et al., 2007). Furthermore, reoxygenation can cause oxidative damage due to the surge of the reactive oxygen species (ROS) from the mitochondrial electron transport system (ETS) (Andrienko et al., 2017; Jastroch et al., 2010). Oxidative stress is considered a hallmark of the hypoxia-reoxygenation (H/R) injury in hypoxia-sensitive organisms such as terrestrial mammals and, if left unchecked, leads to the accumulation of the cellular damage and eventually cell death (Cadenas, 2018; Groehler et al., 2018; Ham and Raju, 2016; Hernansanz-Agustín et al., 2014). Studies in hypoxia-tolerant animals such as the freshwater turtles, crucian carp, and intertidal mollusks and fish uncovered several putative mitochondrial mechanisms that can mitigate oxidative stress during hypoxia-reoxygenation. These include upregulation of antioxidants, suppression of the pathways channeling electrons to ubiquinone, and upregulation of the mitochondrial quality

control mechanisms (including mitochondrial proteases and heat shock proteins) that can repair the damage or prevent aggregation of the damaged proteins (Sokolova, 2018; Sokolova et al., 2019b). However, it remains unknown to what degree these mechanisms are effective in limiting the cellular and tissue damage caused by hypoxia-reoxygenation and preventing the negative outcomes of excessive oxidative stress (such as apoptosis and inflammation) in hypoxia-tolerant organisms.

Studies in the model organisms such as terrestrial mammals, *Drosophila* and *C. elegans* highlighted the important role of autophagy and apoptosis in cellular response to hypoxia-reoxygenation, which may be beneficial or detrimental depending on the intracellular conditions and the extent of autophagy and apoptosis (Ham and Raju, 2016; Lin et al., 2018; Sciarretta et al., 2011; Zhou et al., 2017). Autophagy is a catabolic processes involved in recycling of long-lived proteins and organelles in the cell as a part of the normal cell maintenance (Bialik et al., 2018). Under the hypoxic conditions, when the cells experience energy and nutrient deficiency, the autophagic processes are activated providing substrates for anaerobic ATP production and removing superfluous or damaged intracellular structures (Lin et al., 2018; Solaini et al., 2010). However, during reoxygenation, oxidative stress, calcium overload and mitochondrial dysfunction lead to a major increase of autophagy which may result in tissue injury in the hypoxia-sensitive organisms such as terrestrial mammals (Ham and Raju, 2016; Lin et al., 2018; Sciarretta et al., 2011). Apoptosis (or Type I cell death) also plays a key role in the tissue injury caused by H/R stress. Apoptosis is induced during reoxygenation in response to the oxidative damage caused by the elevated ROS production (Eefting et al., 2004; Wu et al., 2018). Apoptotic cell death plays an important role in mitigating tissue inflammation (which might be caused if the cell died in the less controlled way via necrosis) yet it results in the cell loss and functional impairment of the tissue, so that the extent of tissue apoptosis negatively correlates with the survival and recovery in hypoxia-sensitive organisms such as terrestrial mammals (Blomgren et al., 2003; Eefting et al., 2004). Regulation of autophagy and apoptosis during hypoxia-reoxygenation therefore appears to be an important tolerance mechanism and a potential target for selection in the organisms adapted to frequent oxygen fluctuations such as intertidal bivalves. However, the effects of fluctuating oxygen conditions on tissue levels of apoptosis and autophagy are not yet well understood in hypoxia-tolerant intertidal invertebrates.

Marine intertidal bivalves such as the Pacific oysters *Crassostrea gigas* and the blue mussels *Mytilus edulis* are common organisms in the intertidal, estuarine and shallow coastal habitats in the Northern Hemisphere where they can be exposed to frequent oxygen fluctuations ranging from near-anoxia to hyperoxia during the diurnal and tidal cycles as well as to seasonal hypoxia (Breitburg et al., 2015; de Zwaan and Putzer, 1985; Diaz and Rosenberg, 2008; Richards, 2011). Of these two species, the Pacific oysters are considered more tolerant to abiotic stressors including prolonged hypoxia than the blue mussels (David et al., 2005; Le Moullac et al., 2007; Meng et al., 2018; Zhang et al., 2012; Zhang et al., 2016). Our recent study showed that *C. gigas* survives longer in severe hypoxia and is better at maintaining the intracellular homeostasis of intermediate

metabolites (including the free amino acids, urea cycle and purine metabolism intermediates) during hypoxia-reoxygenation than *M. edulis* (Haider, Falfushynska, Timm and Sokolova, unpublished results). Therefore, we hypothesized that the higher tolerance to H/R stress of *C. gigas* will be reflected in the lower activation of autophagic, apoptotic and inflammatory pathways compared with the less stress-tolerant *M. edulis*. To test this hypothesis, we determined the effects of short-term (1 day) and long-term (6 days) severe hypoxia and post-hypoxic recovery (1 h) on the lysosomal membrane stability, activity of a key autophagic enzyme (cathepsin D) and mRNA expression of the genes involved in the cellular survival and inflammation pathways, including caspases 2, 3 and 8, Bcl-2, BAX, TGF-β-activated kinase 1 (TAK1), nuclear factor kappa B-1 (NF-κB), and two NF-κB activating kinases - the inhibitor of NF-κB kinase subunit α (IKKα) and serine/threonine-protein kinase TBK1-like (TBK1), in *M. edulis* and *C. gigas*. Our study demonstrates that the more tolerant of the two studied species (*C. gigas*) shows blunted or delayed inflammatory and apoptotic response to hypoxia and reoxygenation compared with the less hypoxia-tolerant *M. edulis*. These findings indicate the importance of the regulation of the cell survival pathways in the tolerance to intermitted hypoxia in marine bivalves and demonstrate the utility of the molecular markers of apoptosis, inflammation and autophagy in sentinel marine bivalves for monitoring of the hypoxia-induced stress in estuarine and coastal habitats.

## MATERIALS AND METHODS

***Chemicals.*** Unless indicated otherwise, all chemicals were purchased from Sigma Aldrich (Merck KGaA, Darmstadt, Germany), Carl Roth (Karlsruhe, Germany) or Thermo Fisher Scientific (Schwerte, Germany), and were of the analytical grade or higher.

***Animal collection and care.*** Blue mussels *Mytilus edulis* were from submerged piles in an atidal zone near Warnemünde in the Baltic Sea (54°10′49.602"N, 12°05′21.991"E). The mussels are permanently submerged in this habitat. The Pacific oysters *Crasosstreas gigas* were gathered in the low intertidal zone of the island of List/Sylt in the German Wadden Sea (55°02'54.4"N 8°27'12.6"E). Depending on the tidal phase, these animals experience 1-3 h of emersion per day (M. Wegner, personal communication). All animals were transported within 12 h of collection to the University of Rostock in coolers lined with the seawater-soaked paper towels. The shells were cleaned from epibionts, and the bivalves were kept in aquaria with aerated artificial sea water (ASW) (Instant Ocean ®, Aquarium Systems, Sarrebourg, France) at 15 ± 1 °C for at least four weeks prior to the experiments. Acclimation temperature was similar to the habitat water temperatures (12-16°C). During acclimation and all exposures, salinity was maintained at 15 ± 1 and 30 ± 1 practical salinity units for the mussels and oysters, respectively, which was within 2-4 salinity units of the habitat salinities of these species at the time of collection. Mollusks were fed *ad libitum* by continuous addition of a commercial algal blend (DT's Live Marine Phytoplankton, CoralSands, Wiesbaden, Germany) to experimental tanks according to the manufacturer's instructions.

Bivalves were subjected to severe hypoxia (>0.5% air saturation, >0.01% $O_2$) in air-tight plastic chambers filled with ASW at the respective acclimation salinity (five bivalves in 6 L ASW). The water in the chambers was bubbled with nitrogen until oxygen levels dropped below 0.5% of air saturation. Oxygen content of seawater was measured using a fiber optic oxygen sensor connected to a FireSting$O_2$ Optical Oxygen Meter (PyroScience GmbH, Aachen, Germany). The chamber was submerged in the temperature-controlled aquarium to maintain temperature at 15 ± 0.5 °C. The animals were exposed to a short-term (1 day) or long-term (6 days) hypoxia. Extreme hypoxia such as used in the present study, leads to the valve closure and cessation of feeding in bivalves; therefore, the phytoplankton blend was not added during hypoxia exposure to prevent excessive bacterial growth. For reoxygenation, a subset of mollusks exposed to 1 and 6 days of hypoxia was placed into a fully aerated aquarium for 1 h prior to tissue isolation. Control animals were maintained in normoxia (>95% air saturation). No mortality was found in the mussels or oysters maintained under the normoxic (control) conditions. All mussels survived one day of hypoxic exposure, and 25% of mussels died after six days of severe hypoxia (N=40). In oysters, no mortality was observed during 1-6 days of hypoxia exposure (N=40).

After experimental exposures, control animals as well as those exposed to hypoxia or reoxygenation were dissected on ice. Hemolymph was withdrawn from the anterior adductor muscle sinus to assess the lysosomal membrane stability of hemocytes as a general stress marker (Moore et al., 2006). The digestive gland was dissected, shock-frozen in liquid nitrogen and stored at −80 °C until further analyses, and the digestive gland tissues were collected for analyses of the biomarkers of lipid peroxidation, activity of cathepsin D, and mRNA expression of the apoptotic and inflammatory genes. The digestive gland was chosen as a key organ involved in the nutrient uptake and energy storage of marine bivalves which plays a key role in the whole-organism bioenergetics (Gosling, 1992; Kennedy et al., 1996). In a pilot analysis, we used a randomized block ANOVA to test for the effects of the exposure chambers on the studied traits; no significant effects were detected ($p > 0.05$), and individual mussels were used as biological replicates in all subsequent analyses (N=6).

***Lysosomal membrane stability.*** Lysosomal membrane stability was determined in hemocyte suspension by the Neutral Red Retention (NRR) assay, which is based on the incorporation of the dye into the lysosomes of living cells (Borenfreund and Puerner, 1985). Hemocytes were collected by centrifugation at 700 × *g* for 10 min, washed using a hemocyte (HC) buffer containing 20 mmol $L^{-1}$ Hepes, 436 mmol $L^{-1}$ NaCl, 53 mmol $L^{-1}$ $MgSO_4$, 10 mmol $L^{-1}$ $CaCl_2$ and 10 mmol $L^{-1}$ KCl, pH 7.3, and enumerated using BrightLine hemacytometer. The hemocytes were resuspended in the HC buffer and diluted to 1 × $10^7$ cells $mL^{-1}$. The hemocyte suspensions were incubated for 2 h with 0.04 % neutral red dye and collected by centrifugation (10 min at 700 × *g).* The neutral red dye was extracted from the hemocytes using 200 µl of an acetic acid: ethanol solution (1:1 vol:vol). The absorbance of the extract was measured at 550 nm and standardized to $10^6$ cells.

***Lipid peroxidation.*** Lipid peroxidation (LPO) was determined in the digestive gland homogenate (1:10 w:v) by the production of the thiobarbituric acid-reactive substances (TBARS) (Ohkawa et al., 1979). The absorbance was determined at 532 nm using a SpectraMax M2 microplate reader (Molecular Devices GmbH, Biberach-an-der-Riß, Germany) with LightPath correction. TBARS concentration was calculated using a molar extinction coefficient of $1.56 \cdot 10^5$ $M^{-1}$ $cm^{-1}$ and expressed as nmol $g^{-1}$ wet mass.

***Cathepsin D activity.*** Cathepsin D (EC 3.4.23.5) activity was determined following incubation the digestive gland homogenate in 0.2 M sodium acetate, pH 3.8 with 1% hemoglobin as a substrate (Dingle et al., 1971). The resulting acid-soluble peptides were detected spectrophotometrically at 280 nm using a SpectraMax M2 microplate reader (Molecular Devices GmbH, Biberach-an-der-Riß, Germany) with LightPath correction. Free cathepsin D activity was assessed in the crude homogenate of the digestive gland tissue without detergent addition, whereas the total cathepsin D activity was measured in an aliquot of the same homogenate treated with Triton X100 (0.25%) to release cathepsin D from the lysosomes. Activities were determined using a standard curve with tyrosine. Enzyme activities were referred to the protein content of the enzyme fraction as nmole tyrosine $min^{-1}$ $g^{-1}$ wet mass.

***mRNA expression of the target genes.*** Total RNA was extracted from the digestive gland tissue using TRI Reagent® (Sigma, St. Louis, MO) according to the manufacturer's protocol. The tissue to the TRI Reagent ratio was kept below 1:10 (w: v). RNA samples (280/260 absorbance ratio > 2.0) were cleaned up from the possible DNA contamination using TURBO DNA-free Kit (Thermo Fisher Scientific, Berlin, Germany) according to the manufacturer's instructions. cDNA was obtained from 2 µg of the total RNA using High Capacity cDNA Reverse Transcription Kit (Thermo Fisher Scientific, Berlin, Germany). Quantitative PCR was carried out using StepOnePlus™ Real-Time PCR System Thermal Cycling Block (Applied Biosystems, Thermo Fisher Scientific, Berlin, Germany) and Biozym Blue S'Green qPCR Mix Separate ROX kit (Biozym Scientific GmbH, Hessisch Oldendorf, Germany) using gene-specific primers (Table 1). Reaction mixtures containing 10 µL of 2× qPCR S'Green BlueMix and ROX additive mixture, 1.6 µL of each forward and reverse primer (to the final concentration of 0.4 µmol $L^{-1}$), 4.8 µL PCR grade water and 2 µL of cDNA sample were added to the wells of 96 well PCR plates, sealed (RT-PCR Seal foil, Roth, Karlsruhe, Germany) and centrifuged to collect the contents and eliminate air bubbles. The cycling parameters were as follows: 95 °C for 10 min to activate the polymerase followed by 40 cycles of 15 s at 95 °C and 60 s at 60 °C. Following the amplification, a melt curve analysis was performed to ensure that only a single PCR product was amplified. In each run, serial dilutions of a cDNA standard were amplified to determine the apparent amplification efficiency $E_a$ (Pfaffl, 2001). In a pilot study, we tested three potential housekeeping genes (the eukaryotic elongation factor 1 (eEF1), tubulin and β-actin) in both studied species and chose the reference gene that showed the least variation among and within the experimental treatment groups (eEF1 for *M. edulis* and β-actin for *C. gigas*). Gene-specific primers for the target and housekeeping genes were designed based on the published sequences from *Mytilus* spp. and *C. gigas*

(Table 1). Putative homology between oyster and mussel sequences for the respective genes identified through the TBLASTN search was confirmed by phylogenetic analysis using neighbor-joining tree based on the maximum composite likelihood distance (Kumar et al., 2008). The expression of the target genes [caspase 2, caspase 3, caspase 8, Bcl-2, BAX, TGF-β-activated kinase 1 (TAK1), nuclear factor kappa B-1 (NF-κB), the inhibitor of NF-κB kinase subunit α (IKKα) and serine/threonine-protein kinase TBK1-like (TBK1)] was normalized against the expression of a housekeeping gene (eEF1 or β-actin in the mussels and oysters, respectively) using the gene-specific $E_a$ values as described elsewhere (Pfaffl, 2001; Sanni et al., 2008).

***Statistics.*** Data were tested for the normal distribution and homogeneity of variances using Shapiro-Wilk and Levine test, respectively. In the case of non-normal distribution, data were normalized using the Box-Cox transformation. Within each species, effects of hypoxia and reoxygenation on the studied traits were tested using one-way ANOVA with the experimental exposure regime as a fixed factor. Tukey's honest Significant Difference (HSD) test was used to determine which pairs of means are significantly different from each other. Principal component analysis (PCA) was used on the raw (non-transformed) data to reduce the dimensionality of the data set and compare the integrated biomarker profiles in different experimental groups. The PCA allows integrating and visualizing the patterns of variation and similarities within a multi-variable data set by transforming the set of correlated variables into a smaller number of the orthogonal (uncorrelated) variables called principal components (Ringnér, 2008). All statistical analyses were conducted using IBM® SPSS® Statistics ver. 22.0.0.0 (IBM Corp., Armonk, NY, USA) and GraphPad Prism ver. 8.02 (GraphPad Software Inc., La Jolla, CA, USA) software. The data are shown as means ± standard error of the means (SEM). The effects were considered significant if the probability of the Type I error ($p$) was less than 0.05.

## RESULTS

***Lysosomal membrane stability.*** Exposure to short-term (24 h) and long-term (6 days) hypoxia resulted in the reduced stability of lysosomal membranes of mussels and oysters as shown by the lower Neutral Red retention in their hemocytes (Fig.1). After 1 h of reoxygenation, the lysosomal membrane stability partially recovered but remained below the respective control levels (Fig. 1A, B) except for oysters recovering after 6 days of hypoxia, where the lysosomal membrane stability of hemocytes returned to the baseline levels (Fig.1A, B).

***Oxidative lesions.*** Tissue levels of TBARS increased during the short-time hypoxia in the mussels and decreased in oysters, recovering back to the control levels after 1 h of reoxygenation (Fig. 1C, D). After long-term (6 days) hypoxia, the TBARS levels were suppressed in the mussels and elevated in oysters. One hour of reoxygenation after long-term (6 days) hypoxia was insufficient to restore the TBARS concentrations back to the baseline levels in either of the two studied species (Fig. 1C, D).

***Cathepsin D activity.*** Total and free cathepsin D activity generally remained near the baseline levels after 1 day of hypoxia and subsequent reoxygenation in mussels and oysters (Fig. 2) albeit a slight increase was found in the total cathepsin D activity after 1 day of hypoxia in mussels (Fig. 2A). Long-term (6 days) hypoxia strongly elevated total and free cathepsin D activity in the digestive gland of mussels and oysters (Fig. 2). Notably, the free cathepsin D activity partially recovered after 1 h reoxygenation following long-term (6 days) hypoxia in oysters but continued to increase in mussels (Fig. 2C, D).

***mRNA expression of target genes.*** In *M. edulis*, H/R stress strongly elevated mRNA expression of apoptotic initiator (caspase 2 and 8) and executor (caspase 3) caspases compared with the control (normoxic) levels (Fig. 3A, C, E). Expression levels of caspase 2 increased ~310-fold after 1 day of hypoxia and ~2100-fold after 1 h of reoxygenation in *M. edulis,* compared with the control levels (Fig. 3A). The upregulation was significant but less pronounced after 6 days of hypoxia and subsequent reoxygenation in *M. edulis* resulting in ~140-fold and ~40-fold increase in the levels of caspase 2 transcripts, respectively (Fig. 3A). In *C. gigas*, caspase 2 mRNA remained at the baseline levels after 1 day of hypoxia and subsequent reoxygenation, and increased by ~1.7-fold after 6 days of hypoxia and reoxygenation (Fig. 3B). Caspase 3 mRNA expression in *M. edulis* was ~2.3-fold higher that the baseline (normoxic) levels following 1 h of recovery from short-term hypoxia, and ~1.8 and 1.7-fold higher than the baseline after long-term hypoxia and subsequent reoxygenation (Fig. 3C). In *C. gigas*, no change in the caspase 3 transcript levels were observed during H/R exposures (Fig. 3D). Compared to normoxia, caspase 8 mRNA levels increased by ~2.9 fold in *M. edulis* exposed to 1 h of reoxygenation after the short-term hypoxia but did not change during the long-term hypoxia and reoxygenation (Fig. 3E). *In C. gigas*, short–term hypoxia and reoxygenation had no effect on caspase 8 mRNA levels, and the long-term hypoxia and reoxygenation led to a ~2.2 and 1.8-fold increase in the levels of caspase 8 transcript, respectively (Fig. 3F).

Transforming growth factor-β-activated kinase 1 (TAK1) mRNA expression did not change in response to H/R exposures in the mussels (Fig. 4A). In the oysters, there was a slight (by ~1.7 fold) but significant elevation of TAK1 mRNA levels after 6 days of hypoxia compared with the normoxic control (Fig. 4B). In *M. edulis*, expression levels of Bcl-2 mRNA increased by ~1.9-fold after 6 days of hypoxia compared to the normoxic baseline but did not change in other experimental treatments (Fig. 4C). In *C. gigas*, long-term (but not short-term) hypoxia and reoxygenation led to elevated mRNA levels of Bcl-2 (by ~2.4 and 2.0 fold, respectively, above the normoxic baseline) (Fig. 4D). Reoxygenation after short-term hypoxia as well as long-term hypoxia and reoxygenation led to increased levels of BAX mRNA (by ~1.9-, 1.6- and 1.8-fold, respectively) in *M. edulis* (Fig. 4E) but not in *C. gigas* (Fig. 4F).

The nuclear factor NF-κB mRNA expression increased during short-term and long-term hypoxia (by ~3.7- and 4.6- fold, respectively) and subsequent reoxygenation (by ~6.0- and 3.3- fold, respectively) in *M. edulis* (Fig. 5A) but not in *C. gigas* (Fig. 5B). In *M. edulis*,

short- and long-term hypoxia suppressed mRNA expression of NF-κB inhibitor kinase subunit α (IKKα) by ~4.0 and 2.2- foldbelow the normoxic baseline, respectively (Fig. 5C). In *M. edulis,* mRNA levels of IKKα were also suppressed by ~5.3-fold below the normoxic baseline after 1 h of reoxygenation following short-term hypoxia. In *C. gigas*, mRNA levels of IKKα were slightly (by ~1.6-fold) but significantly elevated after 6 days of hypoxia but not in any other treatment (Fig. 5D). mRNA levels of serine/threonine kinase TBK1 increased after 6 days of hypoxia in *M. edulis* (by ~1.9-fold) and *C. gigas* (by 1.8-fold) but remained close to the control levels in other treatments (Fig. 5E, F).

***Data integration.*** The PCA analysis integrating all the studied stress biomarkers in the digestive gland of *M. edulis* identified two principal components (PC) jointly explaining 56% of the variation in the data set (Supplementary Table 1). The 1st PC (34% of the total variation) had high negative loadings (<-0.5) for most of the studied apoptotic markers (caspase 3, caspase 8, Bcl-2, and BAX), as well as for TAK1, NF-κB, and TBK1, corresponding to strong negative correlations of the respective variables with PC1. The 2nd PC had high positive loadings (>0.5) of the lysosomal membrane stability marker NRR. The 2nd principal component (22% of the total variation) had high negative loadings of the caspase 2 mRNA expression and tissue TBARS content, and high positive loadings of IKKα and free and total cathepsin D activity (Supplementary Table 1).

In *M. edulis*, the control and hypoxia-exposed groups were clearly separated in the plane of the two first principal components (Fig. 6A). After a day of hypoxic exposure, the biomarker profile showed a strong shift of the hypoxia-exposed group towards more negative values along the PC2 mostly associated with the elevated levels of TBARS and caspase 2 mRNA (Fig. 6B). After 1 h of recovery following the short-term (1 day) hypoxia, the biomarker profile of mussels did not return to the control levels (Fig. 6A); rather, a strong shift along the PC2 was observed, reflecting higher expression of multiple apoptotic and inflammatory markers (Fig. 6B). After 6 days of hypoxia, the position of the hypoxia-exposed group shifted to the more positive values of PC1 and more negative values of PC2 compared with the control (Fig. 6A) reflecting increase in the expression of apoptotic, inflammatory and autophagic markers (Fig. 6B). Similar to the situation found after short-term hypoxia, recovery after the long-term (6 days) hypoxia did not result in the recovery of the baseline (control) biomarker profile in the mussels (Fig. 6A).

The PCA analysis of the stress biomarkers in the digestive gland of *C. gigas* identified two principal components (PC) jointly explaining 70% of the variation in the data set (Supplementary Table 2). The 1st PC (55% of the total variation) had high negative loadings (<-0.5) of caspase 2, caspase 8, Bcl-2, BAX, TAK1, NF-κB, IKKα, TBK1, free and total cathepsin D activity and TBARS. The 2nd principal component (15% of the total variation) had high negative loadings of BAX and NF-κB mRNA expression and high positive loadings of tissue TBARS content (Supplementary Table 2).

In *C. gigas*, short-term (1 day) hypoxia did not result in a major shift in the biomarker profile shown by a large overlap in the position of the control group and the group exposed to one day of hypoxia (Fig. 6C). One hour of reoxygenation following the short-

term hypoxia led to the recovery of the biomarker profile in the digestive gland of oysters to the baseline (control) levels (Fig. 6C). After 6 days of hypoxia exposure, the biomarker profile of the oysters shifted towards the more negative values along the PC1 axis (Fig. 6C), indicating elevated expression of apoptotic, inflammatory and autophagic biomarkers (Fig. 6D). One hour of reoxygenation following six days hypoxia was not sufficient to fully restore the normal biomarker profile in *C. gigas* but a partial recovery occurred shown by a shift towards the control (baseline) values (Fig. 6).

## DISCUSSION

Severe short-term (1 day) and long-term (6 days) hypoxia and subsequent reoxygenation induced different responses in the autophagic, apoptotic and inflammatory pathways in the two studied species of marine bivalves (*M. edulis* and *C. gigas*) with the different degree of hypoxia tolerance. The multivariate PCA analysis showed that in *M. edulis*, both one day and six days of hypoxia led to a major shift in the profile of the cellular stress biomarker compared with the control, and this shift was further exaggerated during reoxygenation (Fig. 6). Unlike the mussels, one day hypoxia in the oysters led to a minor change on the profile of the apoptotic, inflammatory and autophagic biomarkers that quickly recovered after reoxygenation. Furthermore, while the long-term hypoxia induced a shift in the biomarker profile in the oysters, the detailed analysis of individual biomarkers (discussed below) indicates that this shift largely reflects a protective cellular response rather than accumulating damage. One hour reoxygenation was sufficient to ensure a partial recovery of the normal biomarker profile in the oysters even after the long-term (6 days) hypoxia. These data indicate that the oysters are more resistant to the induction of apoptosis, inflammation and tissue injury during hypoxia, which may contribute to higher hypoxia tolerance of the oysters compared with the mussels.

### *Autophagy during hypoxia in the mussels and the oysters*

Hypoxia-reoxygenation stress activated autophagy in the mussels and oysters as shown by an increase in the activity of the cathepsin D in the digestive gland. However, the time course and the extent of autophagy activation was different in the two studied species. In the mussels, a significant increase in the activity of the free cathepsin D during the short-term (1 day) hypoxia was found despite the lack of an increase in the total cathepsin D activity. This indicates a release of existing cathepsin D from the mussels' lysosomes during short-term hypoxia, which was not recovered during subsequent reoxygenation. Unlike the mussels, no release of cathepsin D was found after short-term hypoxia and reoxygenation in oysters.

The long-term (6 days) hypoxia led to a considerable increase in the total and free cathepsin D activity in the mussels and the oysters indicating stimulation of autophagic processes. This finding is consistent with the earlier reports on hypoxia-sensitive

organisms such as mammals and insects that show activation of autophagy for energy supply during prolonged hypoxia/ischemia (Bialik et al., 2018; Ham and Raju, 2016; Sciarretta et al., 2011). While mild stimulation of autophagy is considered protective during H/R stress (Samokhvalov et al., 2008; Zhang et al., 2017), a massive increase in the autophagic activity is detrimental and can lead to apoptosis and autophagy-dependent cell death (Bialik et al., 2018; Sciarretta et al., 2011; Solaini et al., 2010). The latter appears to be the case in the mussels where prolonged hypoxia resulted in ~3.5 and ~6-fold increase in the total cathepsin D activity after 6 days of hypoxia and subsequent reoxygenation, respectively, reaching 36-62 nmol Tyr $min^{-1}$ $g^{-1}$ (compared with 10 nmol Tyr $min^{-1}$ $g^{-1}$ in control). Unlike the mussels, the hypoxia-induced increase in the total cathepsin D was less pronounced in the oysters showing ~2.6-fold increase (to 22 nmol Tyr $min^{-1}$ $g^{-1}$) after 6 days of hypoxia, and a partial recovery after one hour of reoxygenation. This smaller increase in the autophagic enzyme activity might indicate less severe energy deficiency and/or lower degree of tissue damage induced by prolonged hypoxia and reoxygenation in the oysters.

***Effects of severe hypoxia and reoxygenation on apoptotic pathways***

While the activity thresholds separating beneficial from detrimental stimulation of autophagy are not known in marine bivalves, analysis of the apoptosis induction patterns are consistent with the notion of the greater tissue damage during hypoxia-reoxygenation in the mussels compared with the oysters. In *M. edulis*, short-term hypoxia led to a dramatic (~310-fold) increase in the expression of a stress-induced initiator caspase 2 above the normoxic baseline indicating induction of the pathways of intrinsic (stress-induced) apoptosis. This response was further enhanced upon reoxygenation indicated by a ~2100-fold upregulation of caspase 2 expression and a ~2.3-2.9-fold upregulation of caspase 3 and caspase 8 mRNA above the normoxic levels. These findings indicate that post-hypoxic reoxygenation acts as a major activator of both the intrinsic (stress-induced) and extrinsic (death-receptor-induced) apoptosis pathways in the mussels. A stronger activation of apoptotic pathways during reoxygenation (compared with hypoxia/ischemia) is commonly observed in hypoxia-sensitive organisms and tissues such as brain, heart and retina of terrestrial vertebrates (Qin et al., 2004; Shao et al., 2011; Singh et al., 2001; Thornton et al., 2017; Vanden Hoek et al., 2003).

Caspase 2 appears to be the key caspase implicated in apoptosis induced by the short-term hypoxia and reoxygenation in the blue mussels *M. edulis*, similar to the earlier reports on the H/R stress in hypoxia-sensitive vertebrate models (Fava et al., 2012; Qin et al., 2004; Shao et al., 2011; Thornton et al., 2017; Vanden Hoek et al., 2003; Xie et al., 2008). Caspase 2 is a highly conserved initiator caspase activated in response to metabolic imbalance, $Ca^{2+}$ overload or endoplasmic reticulum stress (Fava et al., 2012; Movassagh and Foo, 2008). In the mussels *M. edulis*, upregulation of caspase 2 mRNA can also be caused by toxic stress such as exposure to ZnO nanomaterials (Falfushynska et al., 2019). Caspase 8 (a key initiator caspase of the extrinsic apoptosis initiated by death receptor ligands such as the damage activated molecular patterns released from injured

cells), caspase 3 (the main executor caspase on which the intrinsic and extrinsic apoptotic pathways converge) and a pro-apoptotic regulatory protein BAX are also upregulated during reoxygenation in *M. edulis* albeit to a lesser degree than caspase 2. No increase in the expression of an anti-apoptotic regulator Bcl-2, known for its protective effects during H/R stress (Grunenfelder et al., 2001), was found in *M. edulis* during the short-term hypoxia or reoxygenation. Unlike the mussels, no increase in the apoptotic markers was found during the short-term hypoxia and subsequent reoxygenation in the Pacific oyster *C. gigas*.

The apoptotic signature caused by the long-term (6 days) hypoxia and subsequent reoxygenation in the mussels is qualitatively similar to that found during the short-term H/R stress as shown by upregulation of mRNA expression of caspase 2, caspase 3, and a pro-apoptotic regulator BAX. However, an increase in caspase 2 expression was considerably less pronounced in *M. edulis* after the long-term hypoxia and reoxygenation (~40-140-fold) than during the short-term H/R stress (~310-2100-fold). This might be due to the activation of some cellular protective mechanisms such as the elevated expression of the anti-apoptotic regulator Bcl-2 after prolonged hypoxia in *M. edulis*. Alternatively, this might reflect selective survival of the mussels that show blunted apoptotic response and thus less extensive tissue damage during prolonged hypoxia. Interestingly, the Pacific oysters also showed activation of apoptotic pathways during prolonged hypoxia including ~1.7-2.2-fold increase in the mRNA levels of the initiator caspases 2 and 8. It is not known whether such mild upregulation of the transcript levels has implications for the functional activities of caspases 2 and 8, but this increase indicates an induction of apoptotic signaling pathways in the oysters during long-term hypoxia. Notably, mRNA levels of the executor caspase 3 and the pro-apoptotic regulator BAX did not increase during the prolonged hypoxia in oysters, whereas the mRNA levels of an anti-apoptotic Bcl-2 protein were ~2.4-fold elevated. These results show that the oyster tissues are well protected from apoptosis during prolonged hypoxia and indicate a potential role of Bcl-2 in this protection, similar to the findings in the vertebrate model systems (de Graaf et al., 2002; Grunenfelder et al., 2001; Mattson and Kroemer, 2003; Strasser et al., 2000; Vukosavic et al., 2000). Reoxygenation after the long-term hypoxia did not lead to further activation of the apoptotic pathways in the mussels or the oysters, and the gene expression pattern of the apoptosis-related genes during the 1$^{st}$ hour of recovery was similar to that found after the long-term (6 days) hypoxia.

It is worth noting that oxidative injury is unlikely to be the main trigger of the apoptotic cell death in the digestive gland tissues of the mussels and the oysters exposed to H/R stress. There was no correlation between the accumulation of lipid peroxidation products (TBARS) and the expression of pro-apoptotic genes (including caspases and BAX) in the digestive gland tissue of the mussels shown by the different direction of the respective vectors in the PCA analysis (Fig. 6B). In oysters, accumulation of the lipid peroxidation products coincides with the increase in the expression of apoptotic genes including caspase 2 and 8, and the anti-apoptotic gene Bcl-2. However, comparison across the two studied species does not bear out the hypothesis that the onset of apoptosis is driven by

the oxidative stress, as the strongest upregulation of caspases 2, 3 and 8 (found after the short-time hypoxia and reoxygenation in the mussels) was not associated with accumulation of the oxidative lesions, while a major increase in TBARS (observed after the long-term hypoxia and reoxygenation in the oysters) was associated with a modest increase in caspase 2 and 8, and no increase in caspase 3 expression. Similarly, a decrease in the lysosomal membrane stability caused by H/R stress in the mussels and oysters does not correlate with the degree of stimulation of apoptosis or autophagy within and across the studied species. This indicates that traditional general stress biomarkers (such as lipid peroxidation or lysosomal membrane destabilization) may not be good markers of the tissue injury caused by H/R stress in marine bivalves.

***Inflammatory response to H/R stress***

Apoptosis is considered an important mechanism of limiting inflammatory response to H/R stress (Haanen and Vermes, 1995); however, ineffective clearing of the apoptotic debris as well as accidental (unregulated) cell death can lead to the release of damage activated molecular patterns (DAMPs) resulting in inflammation and bystander injury of surrounding cells (Rovere-Querini et al., 2008; Thornton et al., 2017). Common DAMPs released during H/R stress include DNA, heat shock proteins, ATP, urea or purine metabolites that act as inflammatory signals when found outside their normal cellular compartments (Rovere-Querini et al., 2008; Thornton et al., 2017). A comparative metabolomics study of *M. edulis* and *C. gigas* showed a stronger accumulation of potential DAMPs (such as purine catabolism and urea cycle intermediates) during H/R stress in the tissues of the mussels compared with the oysters (Haider, Falfushynska, Timm, Sokolova, unpublished data). It is not known whether these metabolites are released from the affected cells during H/R stress, but if so, they might contribute to the elevated inflammatory response in the mussels. Thus, elevated mRNA expression of an inflammatory marker NF-κB during H/R stress found in our present study indicates onset of inflammation during the short- and long-term hypoxia and reoxygenation in the mussels, a response that was apparently absent in the oysters. The expression of the inflammatory regulator NF-κB was tightly linked with the induction of apoptosis in *M. edulis* and *C. gigas* as shown by the positive correlation between caspase 2 and NF-κB transcript levels in the mussels ($R=0.40$, $p<0.05$) and the oysters ($R=0.65$, $p<0.001$). This finding agrees with the notion of caspase 2 as a potent activator of NF-κB pathway in marine bivalves including *M. edulis* and *C. gigas* (Falfushynska et al., 2019; Wang et al., 2018).

Transcript levels of NF-κB activating kinases, IKKα and TBK1, showed different response to H/R stress in *M. edulis* and *C. gigas*. In model organisms such as mammals, IKKα and TBK1 induce NF-κB-dependent inflammatory response and can stimulate or suppress apoptosis, depending on the nature of the stimulus (Adli et al., 2010; Chau et al., 2008; Kaltschmidt et al., 2000; Möser et al., 2015; Pomerantz and Baltimore, 1999). IKKα belongs to the catalytic core of IKK complex that activates NF-κB by phosphorylating and inactivating the IκB (inhibitor of kappa B) proteins (Adli et al., 2010). TBK-1 is a non-

canonical IKK that activates NF-κB by phosphorylating an NF-κB activator TANK (Möser et al., 2015). Activation of NF-κB by IKKs initiates transcriptional response of multiple genes involved in inflammation and apoptosis (Adli et al., 2010; Kaltschmidt et al., 2000). The molecular signaling pathways of IKKα and TBK1 are not well studied in marine bivalves but recent analyses show that IKKs of the Pacific oyster *C. gigas* are highly conserved and structurally similar to their vertebrate homologues (Yu et al., 2018) and can activate NF-κB (Escoubas et al., 1999; Huang et al., 2019). Our present study shows that in the mussels, transcriptional upregulation of an inflammatory marker NF-κB during the short-term (1 day) hypoxia and subsequent reoxygenation occurs despite the lack of increase in the TBK1 transcript and suppressed transcription of IKKα. During the long-term (6 days) hypoxia, NF-κB and TBK1 (but not IKKα) mRNA increases in the mussels suggesting propagation of the inflammatory signal. In *C. gigas* IKKα and TBK1 mRNA levels remain unchanged during the short-term hypoxia and show a modest increase during the long-term hypoxia. However, no transcriptional activation of NF-κB is observed during H/R stress in the oysters. Overall, these data indicate an earlier onset of the inflammatory response during H/R stress in the mussels compared with the oysters, and suggest that transcriptional activation of the upstream (IKKα and TBK1) and downstream (NF-κB) components of the inflammatory cascade are not tightly correlated in these two species.

Expression of TAK1, a key intracellular kinase involved in the cross-talk between apoptotic pathways regulated by TGF-β and the inflammatory, NF-κB-dependent pathways (Freudlsperger et al., 2012), was not affected by H/R stress in the mussels and only slightly upregulated during the prolonged hypoxia in the oysters. No correlation was found between TAK1 and NF-κB mRNA expression in the mussels and oysters. This finding is in contrast to the coordinated upregulation of TAK1 and NF-κB mRNA found during exposure of *M. edulis* to ZnO nanoparticles and nanorods (Falfushynska et al., 2019). Taken together, our data and earlier published research indicate that the molecular mechanisms regulating inflammation are stressor-dependent in marine bivalves and may differ during exposure to natural stressors (such as H/R) and anthropogenic contaminants such as ZnO nanomaterials.

### *Conclusions and outlook*

The present study demonstrated strong differences in the patterns of induction of autophagy, apoptosis and inflammation between the two species of marine bivalves with different degree of hypoxia tolerance. The less hypoxia-tolerant of the two studied species, *M. edulis*, showed transcriptional upregulation of key pro-apoptotic and pro-inflammatory genes after one day of hypoxia, accompanied by a strong induction of autophagic enzyme activity after six days of hypoxia. In contrast, the more hypoxia-tolerant *C. gigas* showed muted apoptotic and autophagic response, as well as the lack of increase in the inflammation marker NF-κB during severe hypoxia. A lack of the correlation between the tissue oxidative injury and stimulation of the apoptotic and inflammatory pathways indicates that oxidative stress is not a major underlying

mechanism of the cellular stress response in the studied species, and other mechanisms (such as energy deficiency or negative shifts in the metabolic homeostasis) might be implicated in the induction of apoptosis and inflammation during severe hypoxia. Interestingly, a metabolomics study using animals from the same exposures showed that *C. gigas* is better able to maintain the homeostasis of intermediate metabolites (such as the free amino acids, purine metabolites and urea cycle metabolites) during severe hypoxia and reoxygenation than *M. edulis* (Haider, Falfushynska, Timm, Sokolova, unpublished results). This ability to maintain cellular homeostasis may contribute to the oysters' resistance to apoptosis and inflammation in hypoxia. Future studies using a broader, phylogenetically controlled comparative framework are needed to test this hypothesis and shed new light on the potential role of the resistance to apoptosis and inflammation in the evolution of hypoxia tolerance of marine bivalves. Our study also indicates that expression levels of apoptotic and inflammatory markers (especially the strongly responding genes such as caspase 2 and NF-κB) can serve as useful molecular markers of hypoxia-induced cellular injury in marine bivalves for assessment of the effects of sublethal hypoxic stress as well as the rate of recovery in the coastal populations subjected to periodic oxygen deficiency.

**ACKNOWLEDGEMENTS**

We thank Mathias Wegner (Alfred Wegener Institute Helmholtz Center for Polar and Marine Research, Wadden Sea Station Sylt) for providing oysters for this study. The work was supported by the German Research Foundation (DFG) project MitoBOX (DFG award number 415984732, GZ: SO 1333/5-1) to IMS, and Alexander von Humboldt Fellowship to HF. HP was partially supported by Kent State University Brain Health Institute Pilot Award. The project metadata are available from the PANGAEA® open access database (Sokolova et al., 2019a).

## REFERENCES


**Adli, M., Merkhofer, E., Cogswell, P. and Baldwin, A. S.** (2010). IKKalpha and IKKbeta each function to regulate NF-kappaB activation in the TNF-induced/canonical pathway. *PLoS ONE* **5**, e9428.

**Andrienko, T. N., Pasdois, P., Pereira, G. C., Ovens, M. J. and Halestrap, A. P.** (2017). The role of succinate and ROS in reperfusion injury: A critical appraisal. *Journal of molecular and cellular cardiology* **110**, 1-14.

**Babarro, J. M. F. and De Zwaan, A.** (2008). Anaerobic survival potential of four bivalves from different habitats. A comparative survey. *Comparative Biochemistry and Physiology - Part A: Molecular & Integrative Physiology* **151**, 108-113.

**Bayne, B. L.** (2017). Chapter 6 - Metabolic Expenditure. In *Developments in Aquaculture and Fisheries Science*, vol. 41 (ed. B. Bayne), pp. 331-415: Elsevier.

**Bialik, S., Dasari, S. K. and Kimchi, A.** (2018). Autophagy-dependent cell death – where, how and why a cell eats itself to death. *Journal of Cell Science* **131**, jcs215152.

**Blomgren, K., Zhu, C., Hallin, U. and Hagberg, H.** (2003). Mitochondria and ischemic reperfusion damage in the adult and in the developing brain. *Biochemical and biophysical research communications* **304**, 551-559.

**Borenfreund, E. and Puerner, J. A.** (1985). Toxicity determined in vitro by morphological alterations and neutral red absorption. *Toxicol Lett* **24**, 119-24.

**Breitburg, D., Levin, L. A., Oschlies, A., Grégoire, M., Chavez, F. P., Conley, D. J., Garçon, V., Gilbert, D., Gutiérrez, D., Isensee, K. et al.** (2018). Declining oxygen in the global ocean and coastal waters. *Science* **359**.

**Breitburg, D. L., Hondorp, D., Audemard, C., Carnegie, R. B., Burrell, R. B., Trice, M. and Clark, V.** (2015). Landscape-Level Variation in Disease Susceptibility Related to Shallow-Water Hypoxia. *PLoS ONE* **10**, e0116223.

**Cadenas, S.** (2018). ROS and redox signaling in myocardial ischemia-reperfusion injury and cardioprotection. *Free Radical Biology and Medicine* **117**, 76-89.

**Chau, T. L., Gioia, R., Gatot, J. S., Patrascu, F., Carpentier, I., Chapelle, J. P., O'Neill, L., Beyaert, R., Piette, J. and Chariot, A.** (2008). Are the IKKs and IKK-related kinases TBK1 and IKK-epsilon similarly activated? *Trends Biochem Sci* **33**, 171-80.

**Chu, J. W. F., Curkan, C. and Tunnicliffe, V.** (2018). Drivers of temporal beta diversity of a benthic community in a seasonally hypoxic fjord. *Royal Society Open Science* **5**, 172284.

**David, E., Tanguy, A., Pichavant, K. and Moraga, D.** (2005). Response of the Pacific oyster Crassostrea gigas to hypoxia exposure under experimental conditions. *FEBS Journal* **272**, 5635.

**de Graaf, A. O., Meijerink, J. P. P., van den Heuvel, L. P., DeAbreu, R. A., de Witte, T., Jansen, J. H. and Smeitink, J. A. M.** (2002). Bcl-2 protects against apoptosis induced by antimycin A and bongkrekic acid without restoring cellular ATP levels. *Biochimica et Biophysica Acta (BBA) - Bioenergetics* **1554**, 57-65.

**de Zwaan, A. and Putzer, V.** (1985). Metabolic adaptations of intertidal invertebrates to environmental hypoxia (A comparison of environmental anoxia to exercise anoxia). *In: Physiological Adaptations of Marine Animals. M.S.Laverack [Ed.]. The Company of Biologists Ltd., Cambridge*, 33-62.

**Diaz, R. J. and Rosenberg, R.** (2008). Spreading Dead Zones and Consequences for Marine Ecosystems. *Science* **321**, 926-929.

**Eefting, F., Rensing, B., Wigman, J., Pannekoek, W. J., Liu, W. M., Cramer, M. J., Lips, D. J. and Doevendans, P. A.** (2004). Role of apoptosis in reperfusion injury. *Cardiovascular Research* **61**, 414-426.

**Ellington, W. R.** (1983). The recovery from anaerobic metabolism in invertebrates. *Journal of Experimental Zoology* **228**, 431-444.

**Escoubas, J.-M., Briant, L., Montagnani, C., Hez, S., Devaux, C. and Roch, P.** (1999). Oyster IKK-like protein shares structural and functional properties with its mammalian homologues. *FEBS Letters* **453**, 293-298.

**Falfushynska, H. I., Wu, F., Ye, F., Kasianchuk, N., Dutta, J., Dobretsov, S. and Sokolova, I. M.** (2019). The effects of ZnO nanostructures of different morphology on bioenergetics and stress response biomarkers of the blue mussels Mytilus edulis. *Sci Total Environ* **694**, 133717.

**Fava, L. L., Bock, F. J., Geley, S. and Villunger, A.** (2012). Caspase-2 at a glance. *Journal of Cell Science* **125**, 5911-5915.

**Freudlsperger, C., Bian, Y., Contag Wise, S., Burnett, J., Coupar, J., Yang, X., Chen, Z. and Van Waes, C.** (2012). TGF-β and NF-κB signal pathway cross-talk is mediated through TAK1 and SMAD7 in a subset of head and neck cancers. *Oncogene* **32**, 1549.

**Gosling, E.** (1992). The mussel Mytilus: ecology, physiology, genetics and culture. Developments in aquaculture and fisheries science. Amsterdam: Elsevier.

**Groehler, A., Kren, S., Li, Q., Robledo-Villafane, M., Schmidt, J., Garry, M. and Tretyakova, N.** (2018). Oxidative cross-linking of proteins to DNA following ischemia-reperfusion injury. *Free Radical Biology and Medicine* **120**, 89-101.

**Grunenfelder, J., Miniati, D. N., Murata, S., Falk, V., Hoyt, E. G., Kown, M., Koransky, M. L. and Robbins, R. C.** (2001). Upregulation of Bcl-2 through caspase-3 inhibition ameliorates ischemia/reperfusion injury in rat cardiac allografts. *Circulation* **104**, I202-6.

**Guppy, M. and Withers, P.** (1999). Metabolic depression in animals: physiological perspectives and biochemical generalizations. *Biological Reviews* **74**, 1-40.

**Haanen, C. and Vermes, I.** (1995). Apoptosis and inflammation. *Mediators of inflammation* **4**, 5-15.

**Ham, P. B., 3rd and Raju, R.** (2016). Mitochondrial function in hypoxic ischemic injury and influence of aging. *Prog Neurobiol*.

**Hernansanz-Agustín, P., Izquierdo-Álvarez, A., Sánchez-Gómez, F. J., Ramos, E., Villa-Piña, T., Lamas, S., Bogdanova, A. and Martínez-Ruiz, A.** (2014). Acute hypoxia produces a superoxide burst in cells. *Free Radical Biology and Medicine* **71**, 146-156.

**Hochachka, P. W., Buck, L. T., Doll, C. J. and Land, S. C.** (1996). Unifying theory of hypoxia tolerance: molecular/metabolic defense and rescue mechanisms for surviving oxygen lack. *Proceedings of the National Academy of Sciences of the United States of America* **93**, 9493-9498.

**Hochachka, P. W. and Guppy, M.** (1987). Metabolic arrest and the control of biological time. Cambridge (Ma), London (England): Harvard University Press, 227 pp.

**Hochachka, P. W. and Mommsen, T. P.** (1983). Protons and anaerobiosis. *Science* **219**, 1391-1397.

**Huang, B., Zhang, L., Xu, F., Tang, X., Li, L., Wang, W., Liu, M. and Zhang, G.** (2019). Oyster Versatile IKKα/βs Are Involved in Toll-Like Receptor and RIG-I-Like Receptor Signaling for Innate Immune Response. *Front Immunol* **10**, 1826-1826.

**Jastroch, M., Divakaruni, A. S., Mookerjee, S., Treberg, J. R. and Brand, M. D.** (2010). Mitochondrial proton and electron leaks. *Essays in Biochemistry* **47**, 53-67.

**Kaltschmidt, B., Kaltschmidt, C., Hofmann, T. G., Hehner, S. P., Droge, W. and Schmitz, M. L.** (2000). The pro- or anti-apoptotic function of NF-kappaB is determined by the nature of the apoptotic stimulus. *Eur J Biochem* **267**, 3828-35.

**Kennedy, V. S., Newell, R. I. E., Eble, A. F. and (eds).** (1996). The eastern oyster Crassostrea virginica. College Park ,Maryland: A Maryland Sea Grant Book.

**Kochmann, J., Buschbaum, C., Volkenborn, N. and Reise, K.** (2008). Shift from native mussels to alien oysters: Differential effects of ecosystem engineers. *Journal of Experimental Marine Biology and Ecology* **364**, 1-10.

**Kumar, S., Nei, M., Dudley, J. and Tamura, K.** (2008). MEGA: A biologist-centric software for evolutionary analysis of DNA and protein sequences. *Briefings in Bioinformatics* **9**, 299-306.

**Le Moullac, G., Queau, I., Le Souchu, P., Pouvreau, S., Moal, J., Le Coz, J. R. and Damain, J. F.** (2007). Metabolic adjustments in the oyster *Crassostrea gigas* according to oxygen level and temperature. *Marine Biology Research* **3**, 357-366.

**Levin, L. A., Ekau, W., Gooday, A. J., Jorissen, F., Middelburg, J. J., Naqvi, S. W. A., Neira, C., Rabalais, N. N. and Zhang, J.** (2009). Effects of natural and human-induced hypoxia on coastal benthos. *Biogeosciences* **6**, 2063-2098.

**Lewis, J. M., Costa, I., Val, A. L., Almeida-Val, V. M. F., Gamperl, A. K. and Driedzic, W. R.** (2007). Responses to hypoxia and recovery: repayment of oxygen debt is not associated with compensatory protein synthesis in the Amazonian cichlid, *Astronotus ocellatus*. *Journal of Experimental Biology* **210**, 1935-1943.

**Lin, X. L., Xiao, W. J., Xiao, L. L. and Liu, M. H.** (2018). Molecular mechanisms of autophagy in cardiac ischemia/reperfusion injury (Review). *Mol Med Rep* **18**, 675-683.

**Mattson, M. P. and Kroemer, G.** (2003). Mitochondria in cell death: novel targets for neuroprotection and cardioprotection. *Trends in molecular medicine* **9**, 196-205.

**Meng, J., Wang, T., Li, L. and Zhang, G.** (2018). Inducible variation in anaerobic energy metabolism reflects hypoxia tolerance across the intertidal and subtidal distribution of the Pacific oyster (Crassostrea gigas). *Marine Environmental Research* **138**, 135-143.

**Moore, M. N., Icarus Allen, J. and McVeigh, A.** (2006). Environmental prognostics: An integrated model supporting lysosomal stress responses as predictive biomarkers of animal health status. *Marine Environmental Research* **61**, 278-304.

**Möser, C. V., Stephan, H., Altenrath, K., Kynast, K. L., Russe, O. Q., Olbrich, K., Geisslinger, G. and Niederberger, E.** (2015). TANK-binding kinase 1 (TBK1) modulates inflammatory hyperalgesia by regulating MAP kinases and NF-κB dependent genes. *Journal of Neuroinflammation* **12**, 100.

**Movassagh, M. and Foo, R. S. Y.** (2008). Simplified apoptotic cascades. *Heart Failure Reviews* **13**, 111-119.

**Pomerantz, J. L. and Baltimore, D.** (1999). NF-kappaB activation by a signaling complex containing TRAF2, TANK and TBK1, a novel IKK-related kinase. *EMBO J* **18**, 6694-704.

**Qin, Y., Vanden Hoek, T. L., Wojcik, K., Anderson, T., Li, C.-Q., Shao, Z.-H., Becker, L. B. and Hamann, K. J.** (2004). Caspase-dependent cytochrome c release and cell death in chick cardiomyocytes after simulated ischemia-reperfusion. *AMERICAN JOURNAL OF PHYSIOLOGY-HEART AND CIRCULATORY PHYSIOLOGY* **286**, H2280-H2286.

**Reise, K., Buschbaum, C., Büttger, H., Rick, J. and Wegner, K. M.** (2017). Invasion trajectory of Pacific oysters in the northern Wadden Sea. *Marine Biology* **164**, 68.

**Richards, J. G.** (2011). Physiological, behavioral and biochemical adaptations of intertidal fishes to hypoxia. *J Exp Biol* **214**, 191-9.

**Ringnér, M.** (2008). What is principal component analysis? *Nature Biotechnology* **26**, 303-304.

**Rovere-Querini, P., Brunelli, S., Clementi, E. and Manfredi, A. A.** (2008). Cell Death: Tipping the Balance of Autoimmunity and Tissue Repair. *Current Pharmaceutical Design,* **14**, 269-277.

**Samokhvalov, V., Scott, B. A. and Crowder, C. M.** (2008). Autophagy protects against hypoxic injury in C. elegans. *Autophagy* **4**, 1034-1041.

**Sciarretta, S., Hariharan, N., Monden, Y., Zablocki, D. and Sadoshima, J.** (2011). Is autophagy in response to ischemia and reperfusion protective or detrimental for the heart? *Pediatr Cardiol* **32**, 275-81.

**Shao, Z.-H., Wojcik, K. R., Qin, Y., Li, C.-Q., Hoek, T. L. V. and Hamann, K. J.** (2011). Blockade of Caspase-2 Activity Inhibits Ischemia/Reperfusion-Induced Mitochondrial Reactive Oxygen Burst and Cell Death in Cardiomyocytes. *Journal of Cell Death* **4**, JCD.S6723.

**Shick, J. M., de Zwaan, A. and de Bont, A. M. T.** (1983). Anoxic metabolic rate in the mussel *Mytilus edulis L*. estimated by simultaneous direct calorimetry and biochemical analysis. *Physiological Zoology* **56**, 56-63.

**Singh, M., Savitz, S. I., Hoque, R., Gupta, G., Roth, S., Rosenbaum, Pearl S. and Rosenbaum, D. M.** (2001). Cell-specific caspase expression by different neuronal phenotypes in transient retinal ischemia. *Journal of neurochemistry* **77**, 466-475.

**Sokolova, I.** (2018). Mitochondrial Adaptations to Variable Environments and Their Role in Animals' Stress Tolerance. *Integrative and Comparative Biology* **58**, 519-531.

**Sokolova, I. M., Bock, C. and Pörtner, H. O.** (2000). Resistance to freshwater exposure in White Sea *Littorina* spp. I: Anaerobic metabolism and energetics. *Journal of Comparative Physiology B: Biochemical, Systemic, and Environmental Physiology* **170**, 91-103.

**Sokolova, I. M., Falfushynska, G. I. and H., P.** (2019a). Effects of intermittent hypoxia on the cell survival and inflammatory responses in the intertidal marine bivalves *Mytilus edulis* and *Crassostrea gigas*. In *PANGAEA*. https://doi.org/10.1594/PANGAEA.907769.

**Sokolova, I. M., Sokolov, E. P. and Haider, F.** (2019b). Mitochondrial Mechanisms Underlying Tolerance to Fluctuating Oxygen Conditions: Lessons from Hypoxia-Tolerant Organisms. *Integrative and Comparative Biology*.

**Solaini, G., Baracca, A., Lenaz, G. and Sgarbi, G.** (2010). Hypoxia and mitochondrial oxidative metabolism. *Biochimica et Biophysica Acta (BBA) - Bioenergetics* **1797**, 1171-1177.

**Storey, K. B. and Storey, J. M.** (2004). Metabolic rate depression in animals: transcriptional and translational controls. *Biological Reviews* **79**, 207-233.

**Strasser, A., O'Connor, L. and Dixit, V. M.** (2000). Apoptosis signaling. *Annu Rev Biochem* **69**, 217-45.

**Thornton, C., Leaw, B., Mallard, C., Nair, S., Jinnai, M. and Hagberg, H.** (2017). Cell Death in the Developing Brain after Hypoxia-Ischemia. *Frontiers in Cellular Neuroscience* **11**.

**Vanden Hoek, T. L., Qin, Y., Wojcik, K., Li, C.-Q., Shao, Z.-H., Anderson, T., Becker, L. B. and Hamann, K. J.** (2003). Reperfusion, not simulated ischemia, initiates intrinsic apoptosis injury in chick cardiomyocytes. *AMERICAN JOURNAL OF PHYSIOLOGY-HEART AND CIRCULATORY PHYSIOLOGY* **284**, H141-H150.

**Vukosavic, S., Stefanis, L., Jackson-Lewis, V., Guegan, C., Romero, N., Chen, C., Dubois-Dauphin, M. and Przedborski, S.** (2000). Delaying Caspase Activation by Bcl-2: A Clue to Disease Retardation in a Transgenic Mouse Model of Amyotrophic Lateral Sclerosis. *Journal of Neuroscience [J. NEUROSCI.]* **20**, 9119-9125.

**Wang, F., Yu, Z., Wang, W., Li, Y., Lu, G., Qu, C., Wang, H., Lu, M., Wang, L. and Song, L.** (2018). A novel caspase-associated recruitment domain (CARD) containing protein (CgCARDCP-1) involved in LPS recognition and NF-κB activation in oyster (Crassostrea gigas). *Fish & Shellfish Immunology* **79**, 120-129.

**Wu, M. Y., Yiang, G. T., Liao, W. T., Tsai, A. P. Y., Cheng, Y. L., Cheng, P. W., Li, C. Y. and Li, C. J.** (2018). Current Mechanistic Concepts in Ischemia and Reperfusion Injury. *Cellular Physiology and Biochemistry* **46**, 1650-1667.

**Xie, Y., Niu, Y., Yuan, C., Yang, Y., Zhou, W. and Yu, X.** (2008). Effects of brain-derived neurotrophic factor on the expression of caspase-2 and caspase-3 and cell apoptosis in retinal ischemia/reperfusion injury. *Int J Ophthalmol* **1**, 104-108.

**Yu, M., Chen, J., Bao, Y. and Li, J.** (2018). Genomic analysis of NF-κB signaling pathway reveals its complexity in Crassostrea gigas. *Fish & Shellfish Immunology* **72**, 510-518.

**Zhang, G., Fang, X., Guo, X., Li, L., Luo, R., Xu, F., Yang, P., Zhang, L., Wang, X., Qi, H. et al.** (2012). The oyster genome reveals stress adaptation and complexity of shell formation. *Nature* **490**, 49-54.

**Zhang, G., Li, L., Meng, J., Qi, H., Qu, T., Xu, F. and Zhang, L.** (2016). Molecular Basis for Adaptation of Oysters to Stressful Marine Intertidal Environments. *Annu Rev Anim Biosci* **4**, 357-81.

**Zhang, W., Siraj, S., Zhang, R. and Chen, Q.** (2017). Mitophagy receptor FUNDC1 regulates mitochondrial homeostasis and protects the heart from I/R injury. *Autophagy* **13**, 1080-1081.

**Zhou, X.-Y., Luo, Y., Zhu, Y.-M., Liu, Z.-H., Kent, T. A., Rong, J.-G., Li, W., Qiao, S.-G., Li, M., Ni, Y. et al.** (2017). Inhibition of autophagy blocks cathepsins-tBid-mitochondrial apoptotic signaling pathway via stabilization of lysosomal membrane in ischemic astrocytes. *Cell Death Dis* **8**, e2618.

**FIGURES**

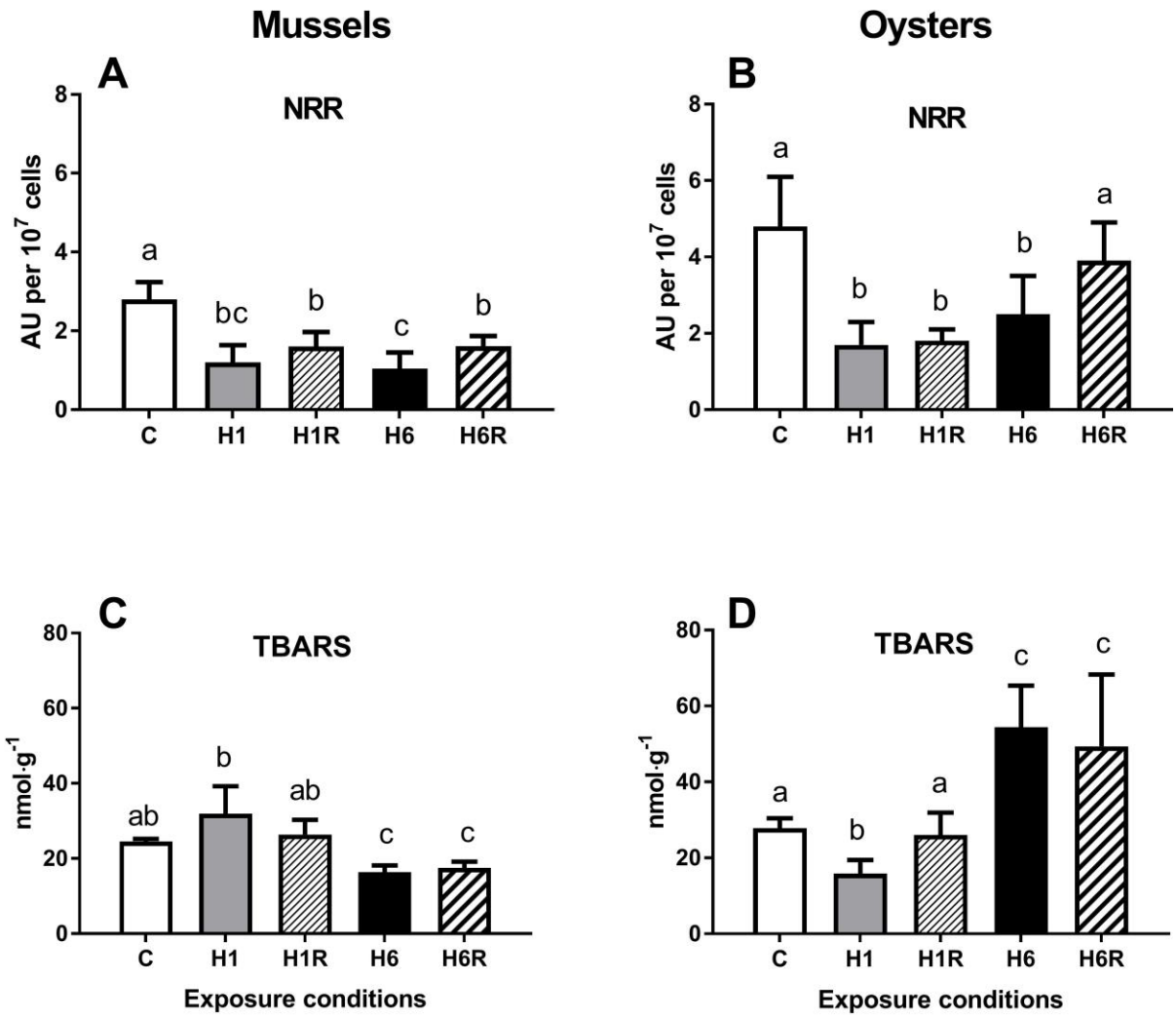


**Figure 1.** Effects of hypoxia and reoxygenation on lysosomal membrane stability and levels of lipid peroxidation in the digestive gland of *M. edulis* and *C. gigas*. A, B – neutral red retention (NRR) as an index of the lysosomal membrane stability in hemocytes; C, D – tissue levels of TBARS.

Experimental groups: H1 – short-term (1 day) hypoxia, H1R - 1 h reoxygenation following the short-term (1 day) hypoxia, H6 - long-term (6 days) hypoxia, H6R - 1 h reoxygenation following the long-term (6 days) hypoxia.

Different letters above columns indicate the values that are significantly different from each other ($p < 0.05$). If two columns share a letter, they are not significantly different ($p > 0.05$). Data are shown as means ± S.D. $N = 6$.

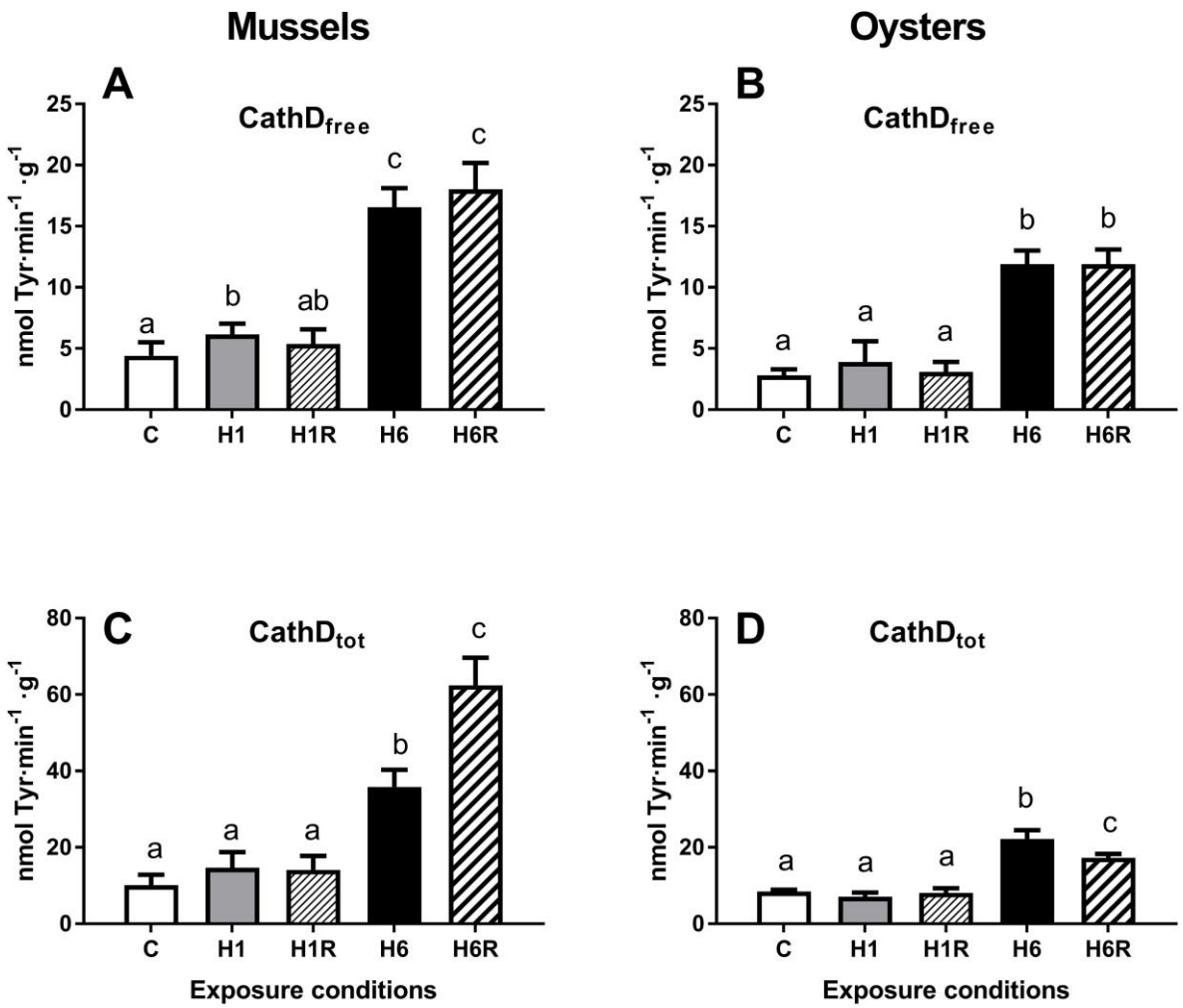


**Figure 2.** Effects of hypoxia and reoxygenation on cathepsin D activity in the digestive gland of *M. edulis* and *C. gigas*.

A, B –activity of the free cathepsin D; C, D – the total activity of cathepsin D.

Experimental groups: H1 – short-term (1 day) hypoxia, H1R - 1 h reoxygenation following the short-term (1 day) hypoxia, H6 - long-term (6 days) hypoxia, H6R - 1 h reoxygenation following the long-term (6 days) hypoxia.

Different letters above columns indicate the values that are significantly different from each other ($p < 0.05$). If two columns share a letter, they are not significantly different ($p > 0.05$). Data are shown as means ± S.D. $N = 6$.

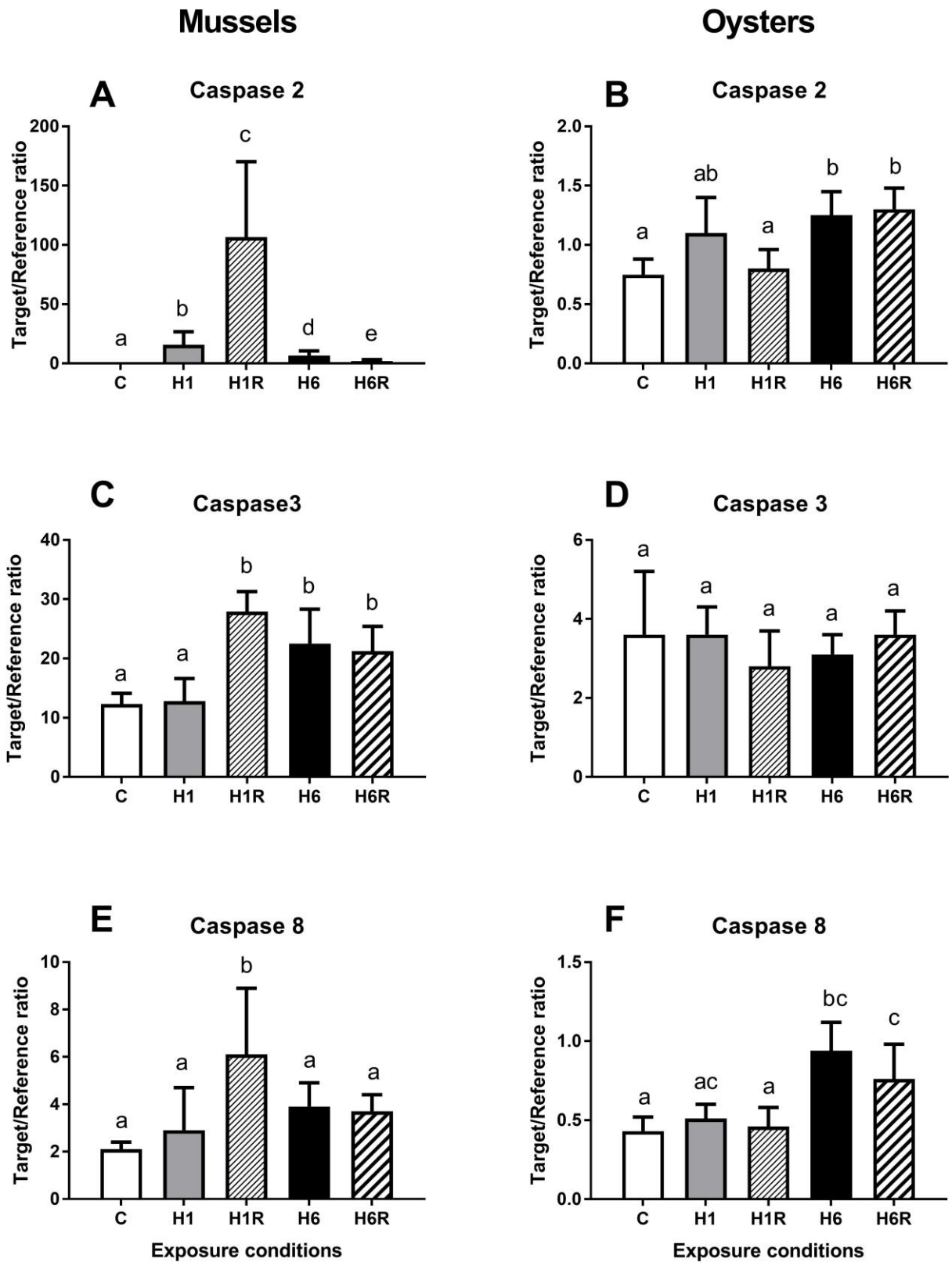


**Figure 3.** Effects of hypoxia and reoxygenation on mRNA expression of the caspases family genes in the digestive gland of *M. edulis* and *C. gigas*.

A, B – expression of caspase 2, C, D – expression of caspase 3, E, F - expression of caspase 8.

Experimental groups: H1 – short-term (1 day) hypoxia, H1R - 1 h reoxygenation following the short-term (1 day) hypoxia, H6 - long-term (6 days) hypoxia, H6R - 1 h reoxygenation following the long-term (6 days) hypoxia.

Different letters above columns indicate the values that are significantly different from each other ($p < 0.05$). If two columns share a letter, they are not significantly different ($p > 0.05$). Data are shown as means ± S.D. $N = 6$.

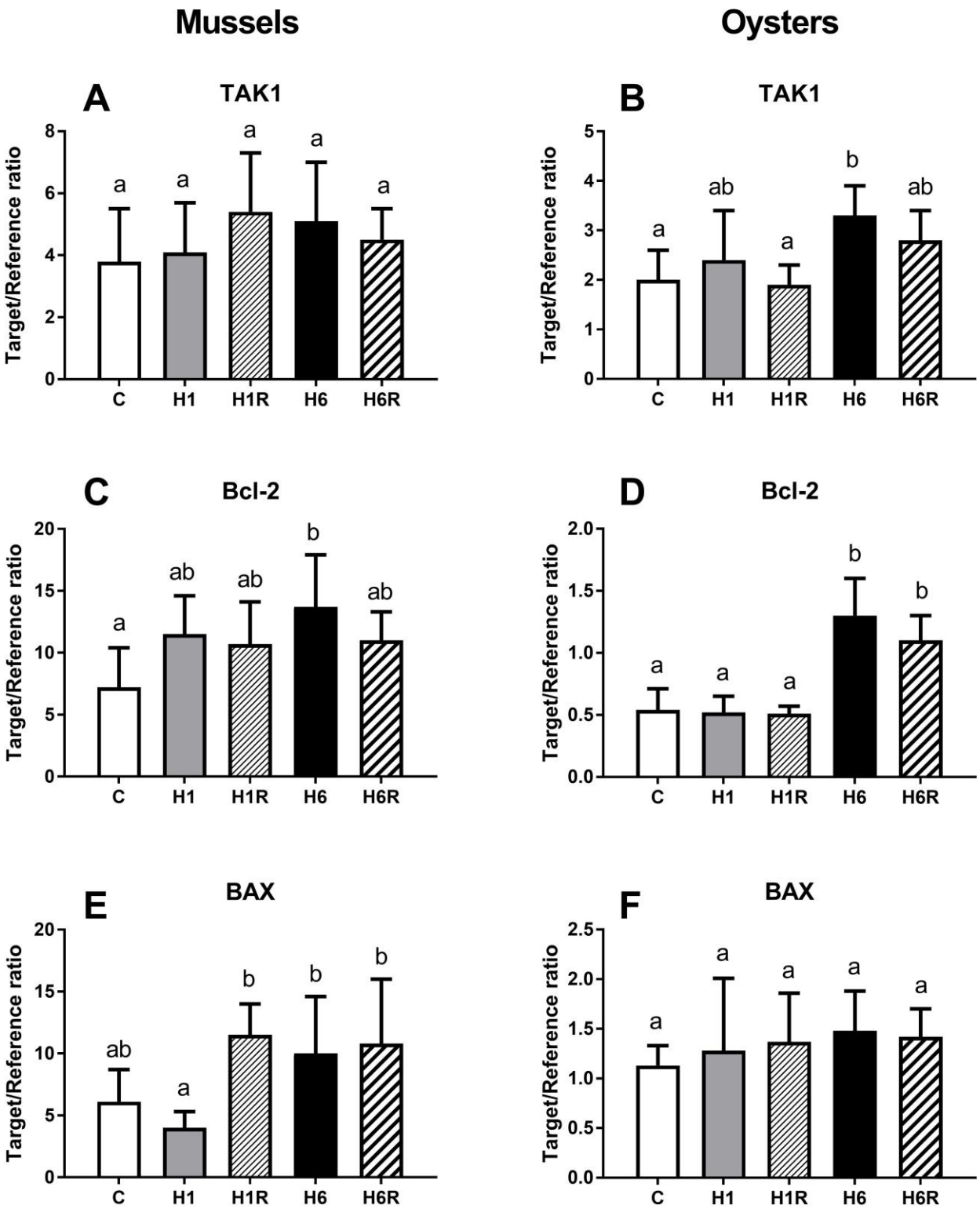


**Figure 4.** Effects of hypoxia and reoxygenation on mRNA expression of the target genes involved in apoptosis pathways in the digestive gland of *M. edulis* and *C. gigas*.

A, B – expression of TAK1, C, D – expression of Bcl-2, E, F - expression of BAX.

Experimental groups: H1 – short-term (1 day) hypoxia, H1R - 1 h reoxygenation following the short-term (1 day) hypoxia, H6 - long-term (6 days) hypoxia, H6R - 1 h reoxygenation following the long-term (6 days) hypoxia.

Different letters above columns indicate the values that are significantly different from each other ($p < 0.05$). If two columns share a letter, they are not significantly different ($p > 0.05$). Data are shown as means ± S.D. $N = 6$.

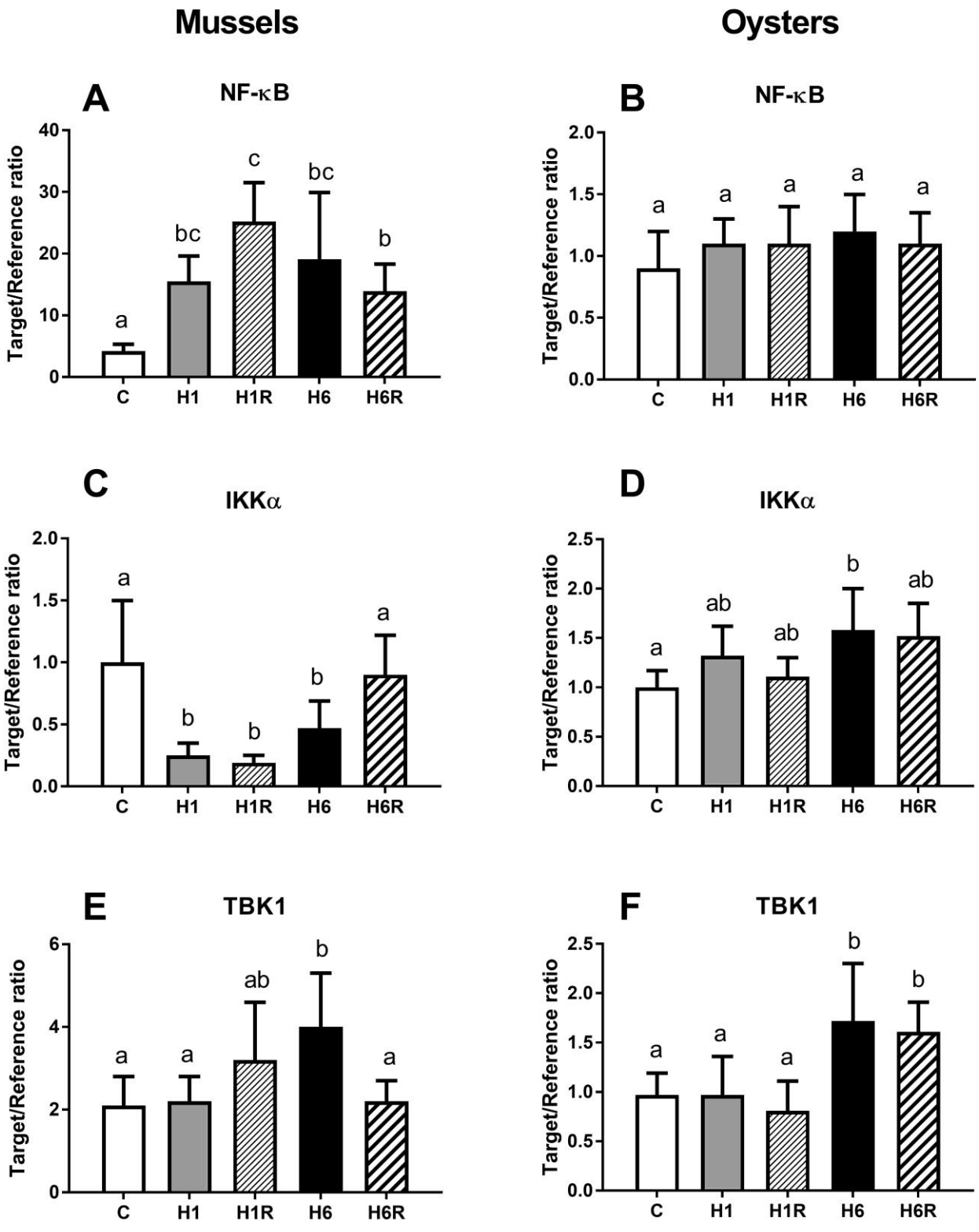


**Figure 5.** Effects of hypoxia and reoxygenation on mRNA expression of the target genes involved in inflammation signaling pathways in the digestive gland of *M. edulis* and *C. gigas*.

A, B –expression of NF-κB, C, D – expression of IKKα, E, F - expression of TBK1.

Experimental groups: H1 – short-term (1 day) hypoxia, H1R - 1 h reoxygenation following the short-term (1 day) hypoxia, H6 - long-term (6 days) hypoxia, H6R - 1 h reoxygenation following the long-term (6 days) hypoxia.

Different letters above columns indicate the values that are significantly different from each other ($p < 0.05$). If two columns share a letter, they are not significantly different ($p > 0.05$). Data are shown as means ± S.D. $N = 6$.

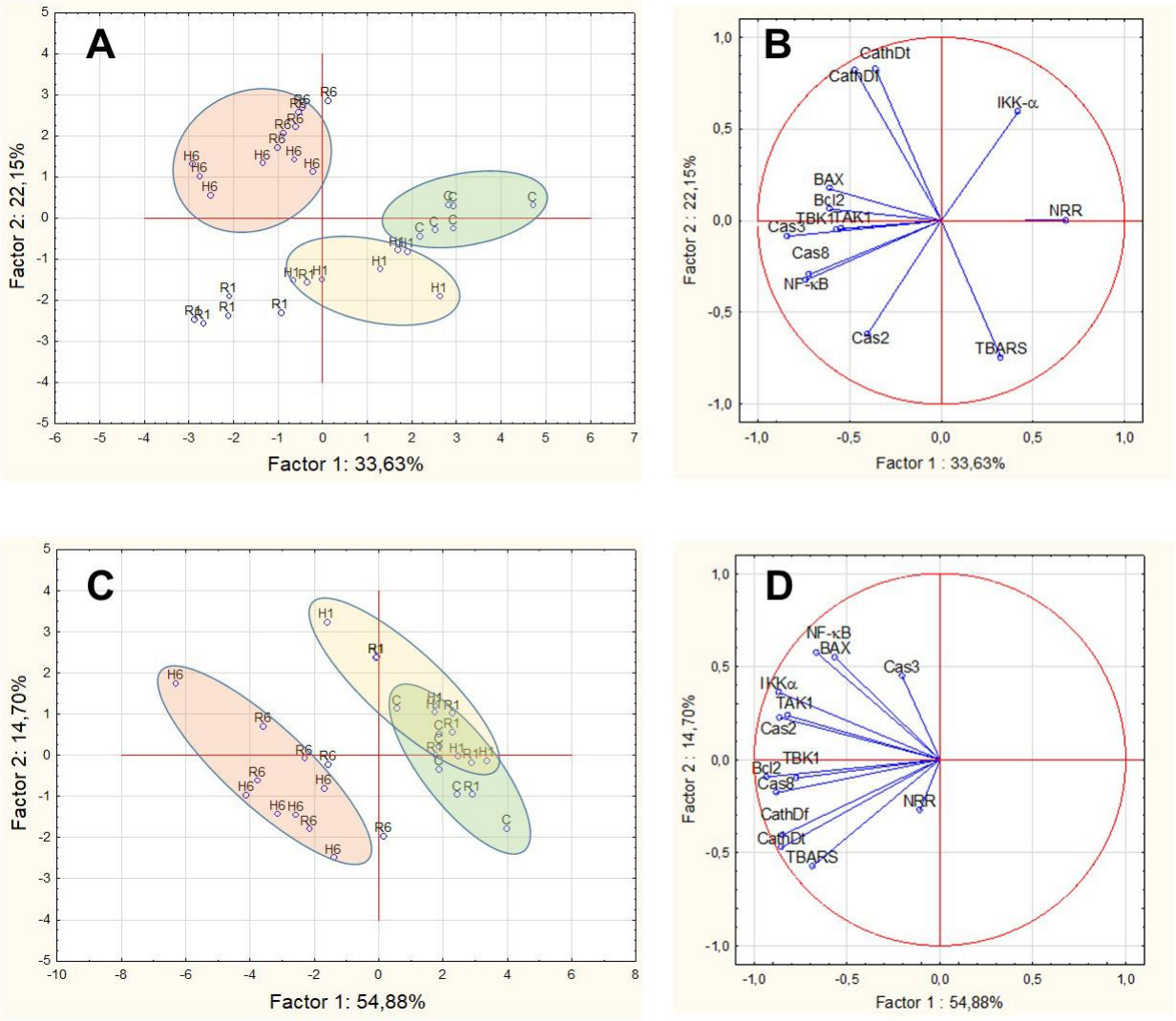


**Figure 6.** PCA score plots (A, C) and variable loading plots (B, D) based on the studied biomarkers from *M. edulis* (A, B) and *C. gigas* (C, D) under hypoxia/reoxygenation stress.

A, C – position of the individual samples from different experimental group in the coordinate plane of 1st two principal components. Experimental groups: H1 – short-term (1 day) hypoxia, R1 - 1 h reoxygenation following the short-term (1 day) hypoxia, H6 - long-term (6 days) hypoxia, R6 - 1 h reoxygenation following the long-term (6 days) hypoxia. Colored ovals mark the clusters of samples from the control (green), 1 day of hypoxia (yellow) and 6 days of hypoxia (orange) groups. Horizontal axis corresponds to the PC1, and the vertical axis – to the PC2.

B, D – variable loading plots showing how much weight different biomarkers have on each of the two 1st principal components. Horizontal axis corresponds to the PC1, and the vertical axis – to the PC2. When the vectors corresponding to different variables (i.e. biomarker values) are close, the two variables are positively correlated. Orthogonal vectors (i.e. forming an angle close to 90°) indicate that the respective variables are not correlated. Biomarker abbreviations: NRR - neutral red retention, CathDt - total cathepsin

D; CathDf - free cathepsin D;  Cas2 – caspase 2; Cas3 – caspase 3; Cas8 – caspase 8; TAK1 - TGF-β-activated kinase 1; Bcl2 - B-cell lymphoma 2, BAX - bcl-2-like protein 4; IKKα - inhibitor of NF-κB kinase subunit α; TBK1 - serine/threonine-protein kinase TBK1-like.

**Table 1.** Primers used for RT-PCR of the target stress-related genes in *M. edulis* and *C. gigas*.

Gene abbreviations: Bcl-2 - B-cell lymphoma 2; BAX - Bcl-2-associated X protein; TAK1 - TGF-β-activated kinase 1; NF-κB – nuclear factor κB (p100/p105); IKKα - inhibitor of NF-κB kinase subunit α; TBK1 - serine/threonine-protein kinase TBK1; EF1 – eukaryotic elongation factor 1α. Because *M. edulis* does not yet have a completely sequenced genome assembly, we used homologous sequences from either *M. galloprovincialis* or *M. edulis* to generate primers.

| Gene | Forward primer (3′-5′) | Reverse primer (3′-5′) | NCBI accession # |
|---|---|---|---|
| ***Mytilus edulis*** | | | |
| Caspase 2 | ACAAGTGCAGATGCTGTGTTG | ACACCTCTCACATTGTCGGC | HQ424449.1 |
| Caspase 3 | ACGACAGCTAGTTCACCAGG | CCACCAGAAGAGGAGTTCCG | HQ424453.1 |
| Caspase 8 | AATGTCGGTACCCCACGATG | CGTGTATGAACCATGCCCCT | HQ424450.1 |
| Bcl-2 | CGGTGGTTGGCAAGGATTTG | CGCCATTGCGCCTATTACAC | KC545829.1 |
| BAX | TAACTGGGGACGTGTAGGCA | CCAGGGGGCGACATAATCTG | KC545830.1 |
| TAK1 | CACCAAACCGAACTGGACCT | GGAACTGCTGTGATCCGACA | KF015298.1 |
| NF-κB | TGGATGATGAGGCCAAACCC | TGAAGTCCACCATGTGACGG | KF051275.1 |
| IKKα | GTGGCCACCAGTCAAGTGAT | TAAGGCTGCAGCTTGCTGAT | KF015301.1 |
| TBK1 | TGCAGGAGCCGATAAAGCAA | CCGCCGGAACAAAATTCCAT | KF015302.1 |
| EF1 | GACAGCAAAAACGACCCACC | TTCTCCAGGGTGGTTCAGGA | AF063420 |
| ***Crassostrea gigas*** | | | |
| Caspase 2 | ACAAACGTGGCCAGATCCAT | ATGATGAGGACCCTGCCTCT | XM_011451515.2 |
| Caspase 3 | GACAGGCTCTTTGACGGACA | ATTTCTCCCATTCGGAGCCC | KR559684.1 |
| Caspase 8 | GTCACATGGTGTGCTCCAGA | CCCGCCAGTCCTGTACATTT | XM_011447144.2 |
| Bcl-2 | AGATTACCGTGCCCTTGTGG | CCGCCTGGAACACTTTGTTG | EU678310.1 |
| BAX | GGATTTACAAGACCCCGGCA | TCATGGTTTGCACTTGGGGT | XM_011426180.2 |
| TAK1 | GGGAGGAGCACGAGTTTGAA | ACAGTTCTGCTGGCATCCTC | XM_011457394.2 |
| NF-κB | GCTACGAGTGTGAGGGGAGATCA | GGGAAACTGATGACGTTGGTGTC | XM_020066072 |
| IKKα | ACCAGGCCGTGAAAAGTCAA | TATACAGCTTCTGCCCACGC | XM_011450699.2 |
| TBK1 | CCAGGACATATACGGTCGCC | TCCCTCGCAACAGACCTCTA | XM_011437045.2 |
| β-Actin | TCCGGAATCCATGAAACATCA | TCCTTTTGCATACGGTCAGC | NM_001308859.1 |

**Table S1.** Principal component (PC) analysis of the stress biomarker profiles in the digestive gland of *M. edulis*.

Variables with high loadings on the respective PC (i.e. with the absolute value of the correlation coefficient >0.5) are highlighted in bold and red.

| PC number | Eigenvalue | % Total variance | Cumulative eigenvalue | Cumulative % |
|---|---|---|---|---|
| 1 | 4,371913 | 33,63010 | 4,37191 | 33,6301 |
| 2 | 2,878956 | 22,14581 | 7,25087 | 55,7759 |
| 3 | 1,461839 | 11,24492 | 8,71271 | 67,0208 |
| 4 | 1,064906 | 8,19159 | 9,77761 | 75,2124 |
| 5 | 0,772798 | 5,94460 | 10,55041 | 81,1570 |
| 6 | 0,655006 | 5,03851 | 11,20542 | 86,1955 |
| 7 | 0,507750 | 3,90577 | 11,71317 | 90,1013 |
| 8 | 0,441991 | 3,39993 | 12,15516 | 93,5012 |
| 9 | 0,312821 | 2,40632 | 12,46798 | 95,9075 |
| 10 | 0,250074 | 1,92365 | 12,71805 | 97,8312 |
| 11 | 0,166488 | 1,28067 | 12,88454 | 99,1119 |
| 12 | 0,082542 | 0,63494 | 12,96708 | 99,7468 |
| 13 | 0,032916 | 0,25320 | 13,00000 | 100,0000 |

| Variable | Factor loadings based on correlations | | |
|---|---|---|---|
| | PC1 | PC 2 | PC3 |
| Caspase 2 | -0,401005 | **-0,618211** | -0,224183 |
| Caspase 3 | **-0,837742** | -0,084785 | -0,181335 |
| Caspase 8 | **-0,717195** | -0,292993 | -0,295436 |
| TAK1 | **-0,565904** | -0,046684 | **-0,504317** |
| NF-κB | **-0,735176** | -0,322469 | 0,229305 |
| Bcl-2 | **-0,608910** | 0,063702 | 0,228400 |
| BAX | **-0,609359** | 0,173613 | **-0,547264** |
| IKKα | 0,419785 | **0,594705** | -0,424704 |
| TBK1 | **-0,543942** | -0,042877 | 0,221162 |
| TBARS | 0,325443 | **-0,746336** | 0,186408 |
| NRR | **0,682777** | 0,001376 | **-0,548485** |
| Cathepsin D total | -0,356237 | **0,823031** | 0,129514 |
| Cathepsin D free | -0,470119 | **0,820646** | 0,226256 |

**Table S2.** Principal component (PC) analysis of the stress biomarker profiles in the digestive gland of *C. gigas*.

Variables with high loadings on the respective PC (i.e. with the absolute value of the correlation coefficient >0.5) are highlighted in bold and red.

| PC number | Eigenvalue | % Total variance | Cumulative Eigenvalue | Cumulative % |
|---|---|---|---|---|
| 1 | 7,134833 | 54,88333 | 7,13483 | 54,8833 |
| 2 | 1,910867 | 14,69897 | 9,04570 | 69,5823 |
| 3 | 1,385330 | 10,65638 | 10,43103 | 80,2387 |
| 4 | 0,695269 | 5,34823 | 11,12630 | 85,5869 |
| 5 | 0,468452 | 3,60347 | 11,59475 | 89,1904 |
| 6 | 0,407127 | 3,13175 | 12,00188 | 92,3221 |
| 7 | 0,305348 | 2,34883 | 12,30723 | 94,6710 |
| 8 | 0,222869 | 1,71438 | 12,53009 | 96,3853 |
| 9 | 0,194611 | 1,49701 | 12,72471 | 97,8824 |
| 10 | 0,130942 | 1,00725 | 12,85565 | 98,8896 |
| 11 | 0,081688 | 0,62837 | 12,93734 | 99,5180 |
| 12 | 0,036101 | 0,27770 | 12,97344 | 99,7957 |
| 13 | 0,026563 | 0,20433 | 13,00000 | 100,0000 |

| Variable | Factor loadings based on correlations | | |
|---|---|---|---|
| | PC1 | PC2 | PC3 |
| Caspase 2 | **-0,862258** | 0,226480 | 0,056310 |
| Caspase 3 | -0,204913 | 0,450020 | **-0,779008** |
| Caspase 8 | **-0,880418** | -0,178410 | 0,137842 |
| TAK1 | **-0,821681** | 0,237215 | 0,063673 |
| NF-κB | **-0,664749** | **0,574869** | -0,010685 |
| Bcl-2 | **-0,932299** | -0,093032 | -0,022755 |
| BAX | **-0,563251** | **0,547934** | 0,196998 |
| IKKα | **-0,866568** | 0,361548 | -0,016142 |
| TBK1 | **-0,773454** | -0,098958 | -0,070868 |
| TBARS | **-0,685870** | **-0,573139** | -0,105592 |
| NRR | -0,108838 | -0,273419 | **-0,831124** |
| Cathepsin D total | **-0,852292** | -0,471557 | 0,065614 |
| Cathepsin D free | **-0,844333** | -0,404317 | 0,036141 |

**Table S1.** Principal component (PC) analysis of the stress biomarker profiles in the digestive gland of *M. edulis*.

Variables with high loadings on the respective PC (i.e. with the absolute value of the correlation coefficient >0.5) are highlighted in bold and red.

| PC number | Eigenvalue | % Total variance | Cumulative eigenvalue | Cumulative % |
|---|---|---|---|---|
| 1 | 4,371913 | 33,63010 | 4,37191 | 33,6301 |
| 2 | 2,878956 | 22,14581 | 7,25087 | 55,7759 |
| 3 | 1,461839 | 11,24492 | 8,71271 | 67,0208 |
| 4 | 1,064906 | 8,19159 | 9,77761 | 75,2124 |
| 5 | 0,772798 | 5,94460 | 10,55041 | 81,1570 |
| 6 | 0,655006 | 5,03851 | 11,20542 | 86,1955 |
| 7 | 0,507750 | 3,90577 | 11,71317 | 90,1013 |
| 8 | 0,441991 | 3,39993 | 12,15516 | 93,5012 |
| 9 | 0,312821 | 2,40632 | 12,46798 | 95,9075 |
| 10 | 0,250074 | 1,92365 | 12,71805 | 97,8312 |
| 11 | 0,166488 | 1,28067 | 12,88454 | 99,1119 |
| 12 | 0,082542 | 0,63494 | 12,96708 | 99,7468 |
| 13 | 0,032916 | 0,25320 | 13,00000 | 100,0000 |

| Variable | Factor loadings based on correlations | | |
|---|---|---|---|
| | PC1 | PC 2 | PC3 |
| Caspase 2 | -0,401005 | **-0,618211** | -0,224183 |
| Caspase 3 | **-0,837742** | -0,084785 | -0,181335 |
| Caspase 8 | **-0,717195** | -0,292993 | -0,295436 |
| TAK1 | **-0,565904** | -0,046684 | **-0,504317** |
| NF-κB | **-0,735176** | -0,322469 | 0,229305 |
| Bcl-2 | **-0,608910** | 0,063702 | 0,228400 |
| BAX | **-0,609359** | 0,173613 | **-0,547264** |
| IKKα | 0,419785 | **0,594705** | -0,424704 |
| TBK1 | **-0,543942** | -0,042877 | 0,221162 |
| TBARS | 0,325443 | **-0,746336** | 0,186408 |
| NRR | **0,682777** | 0,001376 | **-0,548485** |
| Cathepsin D total | -0,356237 | **0,823031** | 0,129514 |
| Cathepsin D free | -0,470119 | **0,820646** | 0,226256 |

**Table S2.** Principal component (PC) analysis of the stress biomarker profiles in the digestive gland of *C. gigas*.

Variables with high loadings on the respective PC (i.e. with the absolute value of the correlation coefficient >0.5) are highlighted in bold and red.

| PC number | Eigenvalue | % Total variance | Cumulative Eigenvalue | Cumulative % |
|---|---|---|---|---|
| 1 | 7,134833 | 54,88333 | 7,13483 | 54,8833 |
| 2 | 1,910867 | 14,69897 | 9,04570 | 69,5823 |
| 3 | 1,385330 | 10,65638 | 10,43103 | 80,2387 |
| 4 | 0,695269 | 5,34823 | 11,12630 | 85,5869 |
| 5 | 0,468452 | 3,60347 | 11,59475 | 89,1904 |
| 6 | 0,407127 | 3,13175 | 12,00188 | 92,3221 |
| 7 | 0,305348 | 2,34883 | 12,30723 | 94,6710 |
| 8 | 0,222869 | 1,71438 | 12,53009 | 96,3853 |
| 9 | 0,194611 | 1,49701 | 12,72471 | 97,8824 |
| 10 | 0,130942 | 1,00725 | 12,85565 | 98,8896 |
| 11 | 0,081688 | 0,62837 | 12,93734 | 99,5180 |
| 12 | 0,036101 | 0,27770 | 12,97344 | 99,7957 |
| 13 | 0,026563 | 0,20433 | 13,00000 | 100,0000 |

| Variable | Factor loadings based on correlations | | |
|---|---|---|---|
| | PC1 | PC2 | PC3 |
| Caspase 2 | **-0,862258** | 0,226480 | 0,056310 |
| Caspase 3 | -0,204913 | 0,450020 | **-0,779008** |
| Caspase 8 | **-0,880418** | -0,178410 | 0,137842 |
| TAK1 | **-0,821681** | 0,237215 | 0,063673 |
| NF-κB | **-0,664749** | **0,574869** | -0,010685 |
| Bcl-2 | **-0,932299** | -0,093032 | -0,022755 |
| BAX | **-0,563251** | **0,547934** | 0,196998 |
| IKKα | **-0,866568** | 0,361548 | -0,016142 |
| TBK1 | **-0,773454** | -0,098958 | -0,070868 |
| TBARS | **-0,685870** | **-0,573139** | -0,105592 |
| NRR | -0,108838 | -0,273419 | **-0,831124** |
| Cathepsin D total | **-0,852292** | -0,471557 | 0,065614 |
| Cathepsin D free | **-0,844333** | -0,404317 | 0,036141 |